

Global biomass fires and infant mortality

Hemant Pullabhotla¹, Mustafa Zahid², Sam Heft-Neal³,
Vaibhav Rathi⁴, Marshall Burke⁵

¹Center on Food Security and the Environment, Stanford University (hemantpk@stanford.edu; @Hpullabhotla)

²Center on Food Security and the Environment, Stanford University (mhzahid@stanford.edu ; @mustafahzahid)

³Center on Food Security and the Environment, Stanford University (sheftneal@stanford.edu; @samheftneal)

⁴Department of Economics, Stockholm University (vaibhav.rathi@iies.su.se; @VaibhavRathi27)

⁵Department of Earth System Science, Stanford University; National Bureau of Economic Research
(mburke@stanford.edu; @MarshallBBurke)

We welcome your feedback on this research. We note that this is a non-peer-reviewed pre-print. The manuscript has been submitted for peer-review at *Nature*. Later versions of this manuscript may include revisions based on peer-review and comments received. If accepted at *Nature* or elsewhere, the final version of this manuscript will be available via the “Peer-reviewed Publication DOI” link on the EarthArXiv page for this paper.

Global biomass fires and infant mortality

Hemant Pullabhotla¹, Mustafa Zahid¹, Sam Heft-Neal¹, Vaibhav Rathi², Marshall Burke^{1,3,4}

¹Center on Food Security and the Environment, Stanford University

²Department of Economics, Stockholm University

³Dept. of Earth System Science, Stanford University

⁴National Bureau of Economic Research

April 14, 2022

1 **Global outdoor biomass burning is a major contributor to air pollution, especially in low**
2 **and middle-income countries.^{1,2} Recent years have witnessed substantial changes in the ex-**
3 **tent of biomass burning, including large declines in Africa.^{3,4} However, direct evidence on**
4 **the contribution of biomass burning to global health outcomes remains limited. Here we**
5 **use georeferenced data on more than 2 million births matched to satellite-derived burned**
6 **area exposure to estimate the burden of biomass fires on infant mortality. We find that each**
7 **additional square kilometer of burning increases infant mortality in nearby downwind loca-**
8 **tions by more than 2%, and we estimate that local biomass burning is responsible for more**
9 **than a third of infant deaths across the tropics where heavy burning is common. This share**
10 **has increased over time due to the rapid decline in other important causes of infant death.**
11 **Applying our model estimates across newly harmonized district-level data covering 98% of**
12 **global infant deaths, we find that exposure to outdoor biomass burning resulted in nearly**
13 **130,000 additional infant deaths per year globally over our 2004-2018 study period. Despite**
14 **the observed decline in biomass burning in Africa, nearly 75% of global infant deaths due**
15 **to burning still occur in Africa. While fully eliminating biomass burning is unlikely, we esti-**
16 **mate that even achievable reductions – equivalent to the lowest observed annual burning in**
17 **each location during our study period – would have avoided more than 70,000 infant deaths**
18 **per year globally since 2004.**

19 Globally, an estimated four million square kilometers of vegetation burns each year.^{5,6} These
20 outdoor biomass fires emit various aerosols, greenhouse gases, and a variety of hazardous trace
21 gases, with significant air quality implications. Biomass fires are estimated to contribute nearly
22 62% of global particulate organic carbon, 27% of black carbon,⁷ 32% of carbon monoxide and
23 40% of carbon dioxide,⁸ and form the single largest source of fine particulate matter (PM_{2.5}) in
24 many developing countries.^{9,10} However, relative contributions of biomass burning to regional
25 air quality depend on the magnitude of emissions from other sources and vary with trends in
26 burning, which show broad regional heterogeneity over the last two decades. For example, Africa
27 has seen an estimated 18.5% decline in the total burned area, 80% of which occurred in North-
28 ern Hemisphere Africa. Conversely, fire activity is estimated to have increased in many areas of
29 South and South-Eastern Asia, likely due to increased adoption of agricultural residue burning
30 practices.^{11,12}

31 Levels and trends in biomass burning are substantially attributable to human activity,^{5,13} either
32 directly, as in tropical regions where land clearing or residue burning is common, or indirectly,
33 as in temperate or boreal forests where anthropogenic climate change is rapidly amplifying wild-
34 fire risk.¹⁴ Given the human role in these fires, their large associated pollutant emissions, the of-
35 ten distant transport of these pollutants into populated areas, and growing evidence from local
36 or regional studies on the health impacts of such burning,^{15–18} understanding the implications
37 of global biomass burning is critical for designing optimal environmental regulations and public
38 health policies.

39 Yet accurately quantifying exposures to smoke from biomass burning and impacts of these expo-
40 sures on health remains challenging, particularly at large spatial scales. First, biomass burning
41 results in a wide variety of emissions, complicating atmospheric model-based approaches to mea-
42 suring the health impacts of burning. Biomass fires result in gases such as carbon dioxide, carbon
43 monoxide, ozone, and nitrogen oxides as well as pollutants such as particulate matter and per-
44 sistent organic pollutants such as polycyclic aromatic hydrocarbons (PAHs) and polychlorinated
45 dibenzo-p-dioxins and dibenzofurans (PCDD/Fs).^{2,19,20} Each of these pollutants is likely to have
46 separate and additive human health impacts through multiple biological channels. Emissions
47 from biomass burning are also poorly constrained empirically, resulting in high levels of uncer-
48 tainty in modeling approaches that use emissions inventories to study impacts.^{21,22} Additionally,
49 to estimate health impacts, modeled emissions are often combined with health dose-response re-
50 lationships that are mainly derived from data in wealthy regions, and these functions might not
51 accurately characterize responses in low and middle-income countries. Consequently, estimates
52 of the health impacts on biomass burning that rely on modeled emission estimates likely provide
53 an incomplete assessment of the actual health costs of exposure to burning.

54 A second challenge is to separate the pollution-driven health impacts of fires from other socioe-
55 conomic factors correlated with fire activity. As noted, vegetation fires are predominantly anthro-
56 pogenic, with more than 90% of overall fire activity estimated to have human-induced causes.^{5,13}
57 Thus accurately quantifying the health impacts of biomass fires requires disentangling the likely
58 negative effects of the pollution they generate from the potential health or livelihood benefits
59 of the economic activity with which they are associated. A few recent studies circumvent these
60 challenges in estimating the impact of fires on health outcomes.^{15–18} However, these studies are
61 limited to narrow geographies. Existing studies at a region or global scale primarily rely on ex-
62 posures from chemical transport model simulations and empirical frameworks that are not well-
63 equipped to isolate health impacts from other co-varying factors.^{10,23,24} Consequently, the global
64 health implications of outdoor biomass burning and its changing patterns in recent years remain
65 unclear.

66 Here we quantify the impact of exposure to biomass burning on infant health by combining satel-
67 lite measures of burned area with geo-located household survey data on infant mortality from na-
68 tionally representative Demographic and Health Surveys (DHS). Our approach of characterizing
69 exposure as observed burned area in the vicinity offers several empirical advantages over using
70 modeled biomass fire emissions. First, it limits the measurement error that could arise from using
71 chemical transport or dispersion models that often rely on uncertain underlying parameterization
72 or emissions inventories.²² Second, our estimated effect reflects the overall impact of exposure
73 to biomass fires, accounting for all varieties of pollutants present in the smoke from vegetative
74 matter combustion. This provides a more accurate assessment of the net health damages from
75 biomass fires rather than the effect of any one single pollutant associated with emissions from
76 fires. An additional advantage of the burned area measure is that it provides a transparent and
77 direct link to an outcome over which policymakers, in principle, could have direct influence.

78 We use infant mortality data from 116 Demographic and Health Surveys representing 54 coun-
79 tries across the developing world and encompassing 2,237,307 births between 2004 to 2018 (Fig
80 1, Extended Data Fig 1). Using survey information on the location and timing of each birth, we
81 estimate exposure to burned biomass during the nine months leading up to and 12 months follow-
82 ing the month of birth (Methods, Extended Data Fig 1,2), the period that existing studies suggest
83 are critical for early life outcomes.²⁵ These data constitute our main sample for estimating the
84 impact of burned area on infant health.

85 To extrapolate derived estimates beyond countries where DHS data are available, we also compile
86 sub-national infant mortality data across 105 countries that fall within the ranges of infant mortal-
87 ity and biomass burned area observed in the estimation sample (Methods, Fig 1). This extended

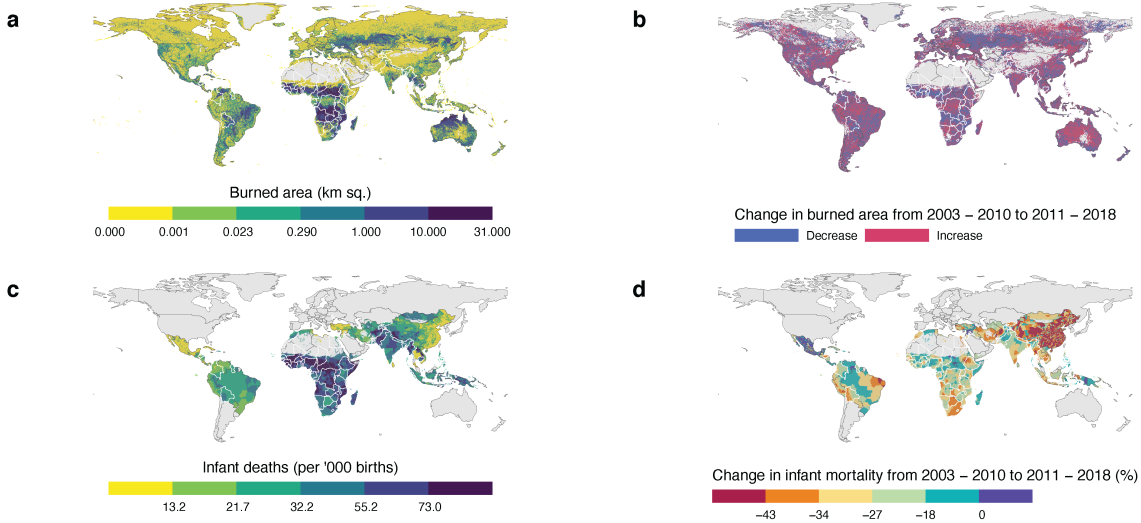


Fig 1. | Global prevalence and change in outdoor vegetation burning and infant mortality (2003 - 2018). (a) Annual average biomass burned area globally 2003 to 2018 (b) Increase or decrease in average burned area between 2003-2010 to 2011-2018 (c) Annual average infant mortality rate (deaths per '000 births) 2003 – 2018. (d) Percentage change in infant mortality from 2003-2010 to 2011-2018. Countries in white borders indicate those with DHS data used in the main estimation. Infant mortality data in c and d are shown for the countries in the extended sample (see Methods) used for calculating global infant mortality attributable to outdoor biomass burning exposure.

88 sample encompasses nearly 98% of the total infant deaths and 80% of total biomass burning ob-
 89 served globally between 2003 and 2018. Using estimates from the DHS sample, we calculate the
 90 infant mortality attributable to biomass burning exposure across these 105 countries, which com-
 91 prise the bulk of the global population exposed to biomass burning and where an overwhelming
 92 majority of infant deaths occur.

93 Exposure to outdoor vegetation burning can increase infant mortality by increasing exposure to
 94 poor air quality. On the other hand, households may derive income and economic benefits from
 95 the activities associated with burning, including preparation or clearing of land for crop or ani-
 96 mal agriculture, the procurement of forest services, or other livelihood activities. To isolate the
 97 air quality component, we leverage changes in wind direction and compare health impacts when
 98 additional area is burned upwind or downwind of a given location (Extended Data Fig 2). While
 99 both upwind and downwind burned areas could influence economic activity, pollution from up-
 100 wind burned areas is more likely to be transported to the birth location and reduce air quality.
 101 We provide supporting evidence for the relatively larger pollution impact from upwind burned
 102 areas (compared to downwind burning) by using data on particulate matter pollution from avail-
 103 able ground monitors situated in low and middle-income countries, matched to up and downwind
 104 burned areas around those monitors.

105 We estimate the effect of exposure to biomass burning on infant mortality using plausibly exoge-
106 nous variation in upwind burned area determined by wind direction changes. Specifically, we
107 compare mortality outcomes for different infants who are born in the same location but, given
108 changes in wind direction and burning activity over time, are exposed to different amounts of
109 upwind burning in the months prior to and post birth. We flexibly account for other seasonal or
110 regionally-trending factors that could be correlated with both variation in burned area and infant
111 mortality, and also include controls for other time-varying local weather conditions (temperature,
112 precipitation, and wind speed) and child, maternal and household characteristics that affect health
113 outcomes (Methods).

114 **Results**

115 We find that that post-birth exposure to biomass burning upwind of birth location increases the
116 risk of infant mortality (Fig 2a). A one square kilometer increase in upwind burned area expo-
117 sure increases infant mortality by 2.1% – an increase of 1.06 (95% confidence interval 0.017 -
118 2.10) additional deaths per '000 births relative to the sample mean infant mortality rate of 52.5
119 deaths per '000 births (Fig 2a, Fig 2c, Extended Data Table 2). Effects are driven by fires that are
120 more proximate to birth locations (Extended Data Fig 4). In contrast to post-birth exposure, we
121 see no effect of in utero exposure to biomass burning on infant mortality (Extended Data Fig 3,
122 Extended Data Table 2). We see positive, albeit noisy, effects of pre-birth exposure (overall, or
123 trimester-wise exposure) on neonatal mortality risk within the first month of birth (Extended Data
124 Fig 4).

125 Outdoor vegetation burning that occurs downwind of a birth location has no impact on the risk
126 of infant mortality (Fig 2a, 2c). The lack of an effect from downwind burning is consistent with
127 an underlying mechanism of biomass burning impacting infant health through deteriorating air
128 quality. To directly test for evidence of this mechanism, we combine data on particulate pollu-
129 tion ($PM_{2.5}$) from nearly 2,000 available ground monitoring stations in low and middle-income
130 countries (Extended Data Fig 5) with measures of upwind and downwind biomass burned area
131 in the vicinity to construct a monthly panel spanning the period 2014 to 2018. Using these data,
132 we estimate the relative impacts of upwind and downwind outdoor biomass burning on $PM_{2.5}$.
133 We see a significant increase in $PM_{2.5}$ at ground station monitors due to upwind burned areas but
134 find no effect of downwind burned areas (Fig 2b). An additional square kilometer of area burned
135 in the upwind direction increases $PM_{2.5}$ by $0.49 \mu g/m^3$ [95% confidence interval 0.05 - 0.93] –
136 an increase of 1% relative to the sample mean of $48.2 \mu g/m^3$ (Fig 2d). Similar to the patterns in
137 infant mortality, upwind burning in a closer vicinity (within 30 km) has a much larger effect on
138 $PM_{2.5}$, relative to burned areas at a further distance (Extended Data Fig 3b, Extended Data Fig
139 6a). These results suggest that changes in air quality are the plausible link between upwind burn-

140 ing and increased infant mortality.

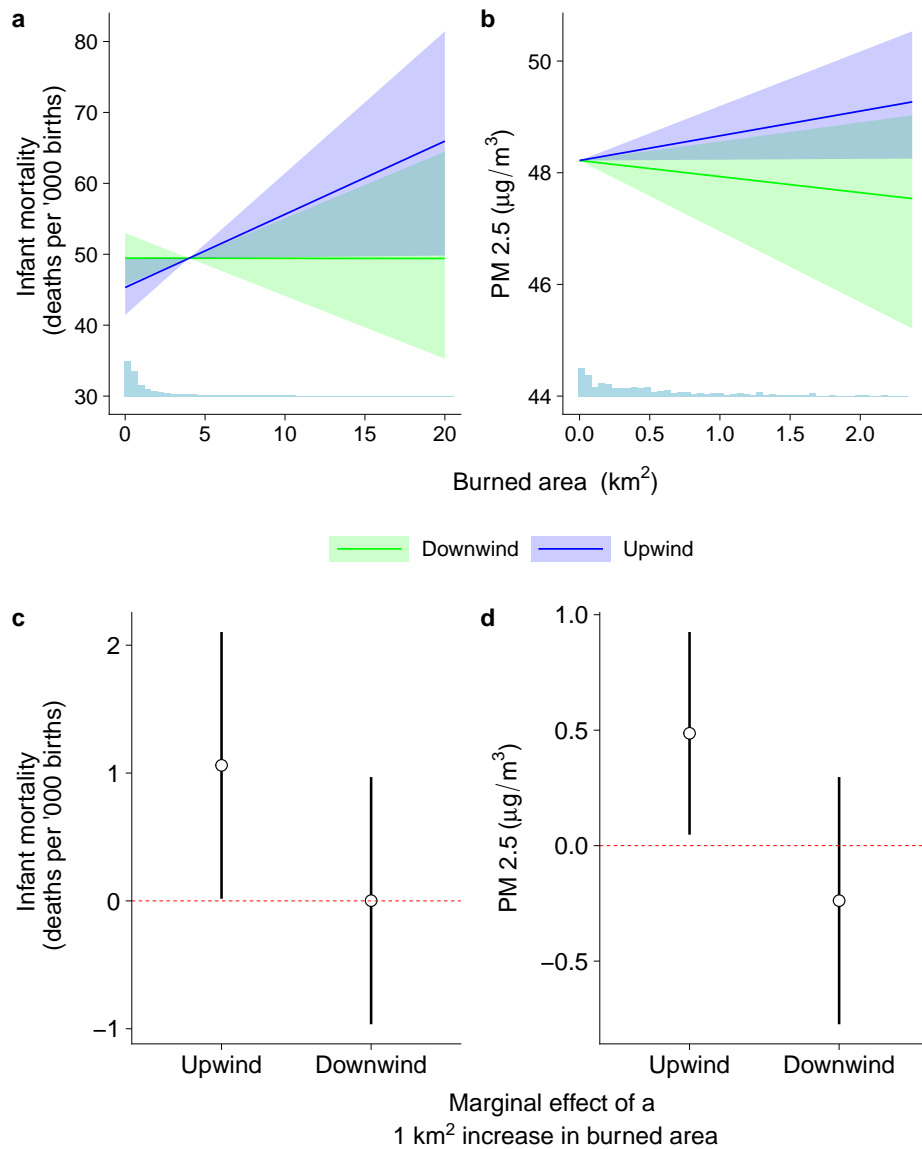


Fig 2. | Impact of up and downwind burned area on infant mortality and particulate matter pollution. Exposure to biomass burning in up-wind direction within 30 km around a location increases **a** infant mortality (IMR) and **b** particulate matter pollution (PM 2.5). **a** and **b** show the response plots (centered at mean of up-wind burned area and outcome variable) for infant mortality (deaths per '000 births) and PM 2.5. Shaded regions in **a** and **b** show the bootstrapped 95% confidence intervals. **c** and **d** shows the marginal effect (coefficients and 95% confidence interval whiskers) of a 1-kilometer square increase in burned area in up and down-wind directions on infant mortality (**c**) and PM 2.5 (**d**). Results shown are based on the regression specification in Equation 1 (Methods). Sample used in **a** and **c** is the DHS births data ($N \approx 2.3$ million) across more than 90,000 locations (Extended Data Fig 1). **b** and **d** use monthly ground station data for nearly 2000 monitors ($N = 10,966$ station-months), largely in Asia and Latin America (Extended Data Fig 5). Up and downwind burned area are based on monthly wind-direction vectors estimated from climate reanalyses data for each location-month (see Methods for details).

141 The estimated effect of exposure to biomass burning on infant mortality remain robust to a vari-
142 ety of alternative models, including models in which differential trends and seasonal effects are
143 allowed to vary sub-nationally across 1- or 2-degree grid cells (Extended Data Table 2) or mod-
144 els that exclude weather variables. Results are also unchanged with the exclusion or inclusion of
145 child, mother, and household characteristics, suggesting that results are unlikely being driven by
146 household-level factors that may be correlated with both infant mortality and exposure to biomass
147 burning (Extended Data Table 2). Finally, the estimates also remain robust to varying the radius
148 used to calculate the exposure to biomass burning (Extended Data Fig 7). The magnitude of the
149 upwind biomass burned area effect declines with an increase in the distance at which burning
150 occurs. These results are strikingly similar to how the effect of upwind burning on PM2.5 con-
151 centrations varies with distance (Extended Data Fig 6b). These results provide additional corrob-
152 oration that exposure to biomass burning affects infant mortality by increasing air pollution.

153 We find that prevailing levels of baseline infant mortality moderate the response to biomass burn-
154 ing exposure (Fig 3a, Extended Data Table 3). An additional square kilometer of burned area has
155 a relatively higher effect on infant mortality in locations with low baseline mortality rates than
156 locations with high baseline infant mortality. This heterogeneity in the infant mortality response
157 is consistent with other evidence^{26,27} and suggests that exposure to smoke from biomass burning
158 is a more prominent risk factor in areas where other risk factors to infant health, such as malaria,
159 pose a lesser threat. Baseline ambient particulate pollution are negatively but not significantly re-
160 lated to the response of infant mortality to burned area exposure (Fig 3b, Extended Data Table 3).
161 We also find no evidence that household wealth helps mitigates the harmful effects of exposure
162 to smoke from outdoor biomass burning (Fig 3c, Extended Data Table 3). Both of these findings
163 are again consistent with earlier evidence that found a linear (rather than concave) dose-response
164 relationship between air pollution exposure and infant health at moderate PM2.5 levels, and found
165 limited evidence for a moderating effect of household wealth.²⁶

166 We combine our estimates from the DHS sample with harmonized infant mortality data from
167 across low- and middle-income countries to estimate the annual number of infant deaths attributable
168 to outdoor biomass fires in the 2004-2018 period. We define attributable deaths as infant deaths
169 that would have been avoided if biomass burning was completely eliminated and calculate them
170 as the difference between the number of model predicted deaths under observed biomass burning
171 conditions and under a hypothetical counterfactual scenario where outdoor biomass burned area
172 was zero. Model results come from the estimation of Equation 3, which accounts for the moder-
173 ating effect of the prevailing baseline infant mortality rate shown in Fig 3a. The statistical model
174 is estimated on the DHS sample and then applied to the expanded sample of 105 low and middle-
175 income countries for which we were able to assemble district-level infant mortality data, limiting

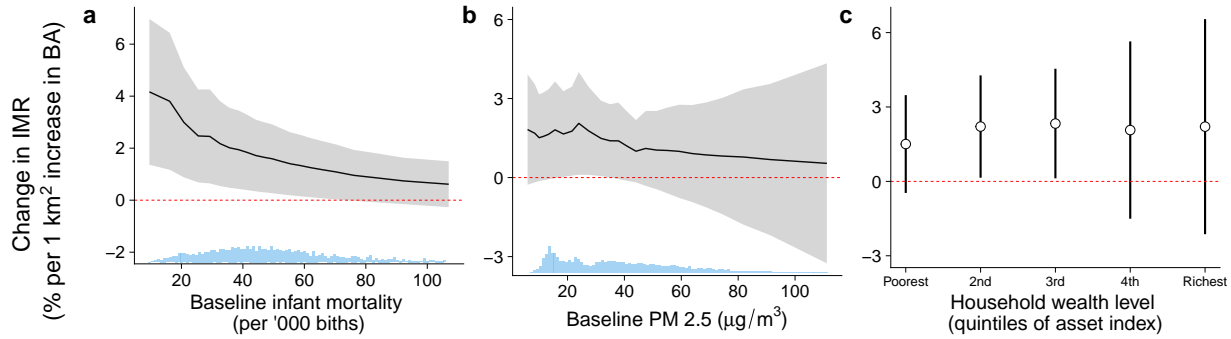


Fig 3. | Heterogeneity in the impact of biomass burning exposure on infant mortality risk across baseline infant mortality, pollution and household wealth. Effect of post-birth up-wind burned area within 30 km across **a** baseline (year prior to birth) levels of infant mortality **b** baseline particulate matter pollution **c** levels of household asset-based wealth index. Histograms on the horizontal axis in panels **a** and **b** show, respectively, the distribution of baseline IMR and PM_{2.5}.

176 the sample in the expanded data to locations that are within the ranges of burned area and infant
 177 mortality observed in the DHS-based estimation sample (Extended Data Fig 10; Methods). Col-
 178 lectively these countries account for 98% of global infant deaths in our sample period and thus
 179 allow us to comprehensively assess the role of biomass burning as a determinant of infant mortal-
 180 ity.

181 We find that, on average, eliminating exposure to smoke from biomass burning would have avoided
 182 nearly 5% of global infant deaths from 2004-2018. This share increases to more than a third in
 183 areas with high levels of exposure to outdoor biomass burning. Regions where this percentage
 184 is the highest include parts of Sub-Saharan Africa, areas around the Amazon basin in Brazil and
 185 equatorial South America, Southeast Asia, and parts of the North China plains (Fig 4a).

186 The temporal patterns in infant mortality attributable to outdoor biomass burning exposure track
 187 observed changes in burned area. Average infant exposure to outdoor biomass burning increased
 188 somewhat in the initial years of the sample period until 2007, and then flattened or declined slightly
 189 through 2018 (Fig 4b). The trend in estimated infant mortality attributable to biomass burning
 190 exposure (Fig 4c) reflects this observed pattern in exposure and is relatively flat at around 1 addi-
 191 tional death per '000 births across all sample years (Fig 4c). While exposure to biomass burned
 192 area and infant mortality attributable to biomass burning exposure have remained relatively sta-
 193 ble, the overall infant mortality rate globally has steadily declined (Fig 4b), thanks in part to
 194 growing incomes and expanded access to health services and technologies. As other contribu-
 195 tors to infant mortality have declined, we estimate that biomass burning-attributable infant deaths
 196 have increased as a share of total infant deaths (Fig 4d), from 2.3% (95% confidence interval 0.23
 197 - 4.28) in 2004 to 3.6% (95% confidence interval 0.74 - 6.50) in 2018.

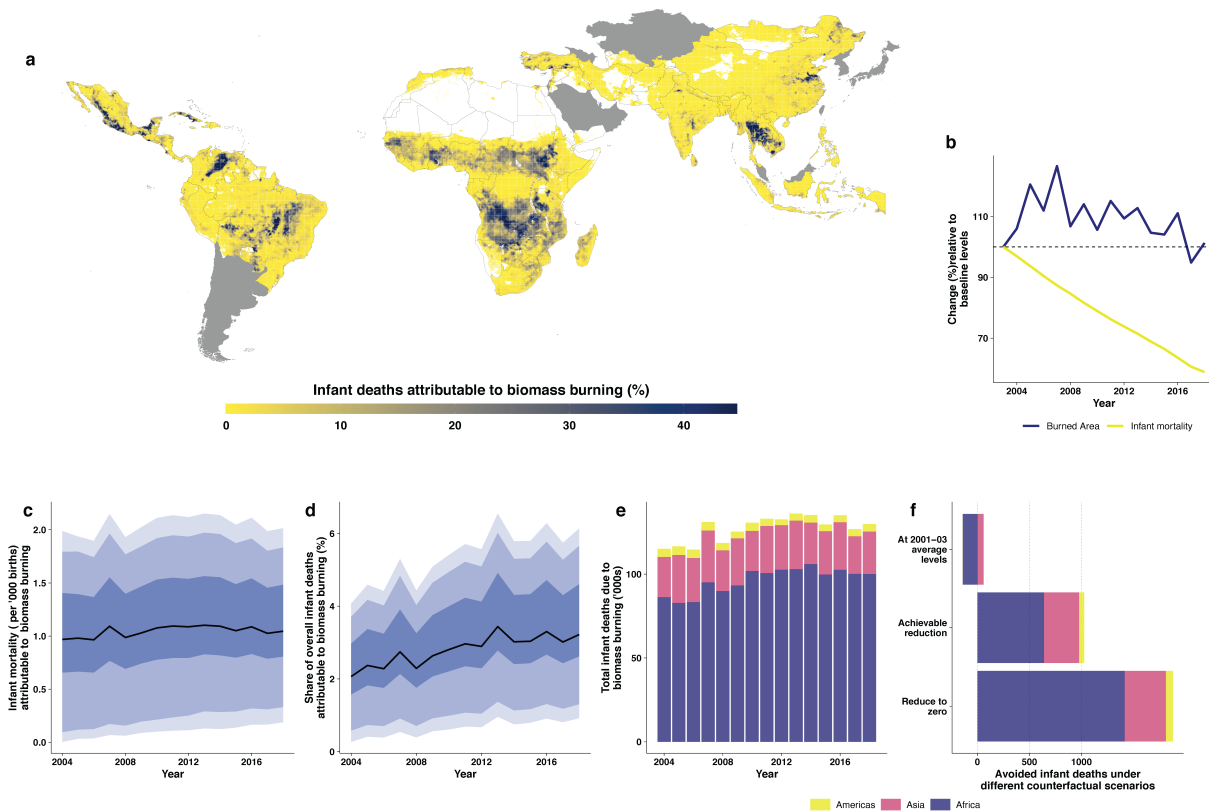


Fig 4. | Avoided infant deaths from reducing post-birth exposure to outdoor biomass burning. **a** Average share of overall infant deaths avoided if biomass burning was reduced to zero over the period 2004 to 2018. **b** Births-weighted annual trends annual trends in infant mortality and burned area as a percentage of baseline levels (2003 infant mortality and 2001-03 average burned area). **c**, **d** and **e**, respectively, show the annual trends in **(c)** births-weighted infant mortality (deaths per '000 births) attributable to biomass burning exposure, **(d)** average infant mortality due to biomass burning exposure as share of overall infant mortality (%), and **(e)** number of avoided infant deaths in '000s by region that result from eliminating biomass burning. **f** shows the total avoided infant deaths (in '000s) under three different scenarios of biomass burning – holding burned area exposure at the baseline observed values, reduction to achievable levels (the minimum observed burned area at each grid cell location during 2004-18), and complete reduction. The colors in the stacked bar charts in **e** and **f** show the break-up of the total infant deaths across three broad regions in the sample – Africa, Asia and the Americas. The solid lines in **c** and **d** show the sample median, and the shaded regions show the 25th to 75th (darkest), 10th to 90th (medium), and 5th to 95th (lightest) percentile ranges based on bootstrapped estimates of predicted infant mortality values at each 1 km X 1 km grid cell, for each year.

198 We estimate that if biomass burning were eliminated entirely, countries across our sample would
199 have experienced a reduction of nearly 130,000 infant deaths on average per year (95% confi-
200 dence interval 26,000 - 237,000). Countries in Africa would have seen the most significant gains
201 in avoided infant deaths, with 98,000 avoided deaths on average per year (95% confidence in-
202 terval 15,000 - 183,000) (Extended Data Fig 10), with an additional average decline per year of
203 27,000 deaths in Asia and 4,600 in Latin America (Fig 4e).

204 These estimates reflect a scenario in which biomass burning is brought down to zero. Because
205 complete elimination in biomass burning may not be possible, we repeat the calculation using
206 an alternate counterfactual scenario where outdoor biomass burned area in each location is held
207 to the lowest observed level in any year for that location – a plausibly achievable reduction. Un-
208 der this reduction scenario, we estimate that 1.1 million infant deaths would have been avoided
209 globally (70,000 per year) since 2004 (Fig 4f). This is roughly 60% of the estimated reduction
210 in infant deaths under the complete elimination of biomass burning suggesting that achievable
211 biomass burning reductions could reduce the overall infant mortality burden by more than half.

212 We also calculate the contribution of recent trends in biomass burning to infant health outcomes
213 by comparing differences in predicted mortality under observed trends versus under a setting
214 where burning was fixed at baseline levels (computed as the three-year average of location-specific
215 burning over 2001-2003). We estimate that observed reductions in burning averted 147,000 infant
216 deaths in Africa and more than 2,000 additional infant deaths in the Americas, relative to a world
217 in which burning was fixed at 2001-2003 levels. On the other hand, because biomass burning in
218 Asia increased over the study period, holding burning at baseline levels would have led to almost
219 61,000 fewer infant deaths in the region over the 2004 - 2018 period (Fig 4f).

220 These regional differences result from the contrasting regional trends in biomass burning wit-
221 nessed in recent years. Biomass burned area has declined substantially in the African region but
222 experienced a modest increase across countries in Asia, relative to the baseline 2001 - 2003 pe-
223 riod (Extended Data Fig 8). In absolute terms, children in our African sample experienced a more
224 than 20% reduction in average upwind burned area, from 4.75 km² per year in 2003 to 3.75 km²
225 by 2018 (Extended Data Fig 9a). During the same period, the infant mortality rate in Africa de-
226 clined from 73 to 45 deaths per 1,000 births (Extended Data Fig 9b), resulting in a reduction in
227 annual all-cause infant deaths from 2.4 million in 2003 to 1.9 million in 2018 (Extended Data Fig
228 9c). Despite a decline in exposure, the overall reduction in infant mortality implies that biomass
229 burning contributes to an increasing share of infant mortality in Africa (Extended Data Fig 10b).
230 Annual infant deaths attributable to biomass burning exposure on the continent continue to re-
231 main around 100,000 deaths per year throughout the sample period (Extended Data Fig 10c). As

232 a result, even though Africa experienced a substantial decrease in exposure compared to other
233 regions, we estimate that nearly 75% of global infant deaths due to burning still occur in Africa.

234 **Discussion**

235 The results of our study complement the limited existing evidence on the effects of biomass burn-
236 ing on overall mortality across all age groups and are broadly consistent with findings from stud-
237 ies focused on early childhood mortality. Quasi-experimental evidence using changes in wind
238 direction similar to the research design in this study finds that agricultural fires contribute to all-
239 cause mortality across all age groups in China,¹⁷ infant mortality in India,¹⁶ and still-birth in
240 Brazil.¹⁵ Our results help expand these regional estimates into a near-global picture of the role
241 of biomass burning on child health.

242 Our results also help confirm findings from studies that use exposure based on chemical transport
243 models (CTMs) combined with dose-response functions from literature to estimate premature
244 deaths in both regional (South-East Asia,²⁸ Brazil,²⁹ and Indonesia³⁰) and global settings.^{10,24}
245 Empirical confirmation of these model-based studies is important, as emissions inventories from
246 biomass burning – a key input into CTM concentration estimates – can have high regional and
247 temporal uncertainty and differ substantially across available products,^{21,31,32} and because exist-
248 ing concentration-response (CR) relationships used to assess health impacts might not accurately
249 capture the specific impact of pollutants emitted during biomass burning.

250 Our estimates are qualitatively similar to comparable findings from this CTM/CR work. For in-
251 stance, from 2016 to 2019, removing anthropogenically set fires was estimated to avoid 265,000
252 global premature deaths annually among children under five¹⁰ – a number comparable to our an-
253 nual estimate of 130,000 deaths among individuals under the age of one. A previous study using
254 cross-country DHS data similar to our estimation sample and relying on within-sibling compar-
255 ison and CTM-based exposure estimated that over the 2000-2014 period, biomass fire exposure
256 contributed to 9 percent of overall child (under-18) mortality in their sample of 55 low-income
257 and middle-income countries.²³ Our estimates suggest that biomass fires contribute to five per-
258 cent of global infant mortality, broadly in agreement with these previous findings, but that contri-
259 butions for infants are substantially higher in a large portion of low income countries.

260 The effects that we find on infant mortality are also supported by growing evidence that prenatal
261 exposure to smoke from fires results in adverse pregnancy and birth outcomes such as preterm
262 birth, pregnancy loss³³ and low birth weights.^{15,34–37} These adverse health impacts at birth could
263 potentially result in a higher risk of infant mortality in the subsequent months. Our results are
264 also consistent with evidence from studies that show exposure to smoke from large wildfires is

265 associated with adverse birth outcomes and increased infant mortality – both in developed^{38–40}
266 as well as low-middle income countries.^{41–44} However, exposure from such fire events tends to
267 result in short, extreme pollution episodes rather than widespread, repeated exposure to less ex-
268 treme but unsafe levels of pollution that accompany the bulk of global fire activity, predominantly
269 caused by seasonal human activities.³

270 Our findings on spatial heterogeneity in the contribution of biomass burning to infant mortality
271 also helps corroborate the regional distribution of mortality estimates found in earlier studies. We
272 find that the contribution of outdoor biomass fires to the overall infant mortality rate is exception-
273 ally high in some low-income locations such as Sub-Saharan Africa, but also high in somewhat
274 higher-income locations with relatively lower overall infant mortality but which are experienc-
275 ing increasing fires – for instance, in Thailand, Laos, Cambodia and other areas of Southeast Asia
276 (Fig 4a, Extended Data Fig 12).⁴⁵ These patterns echo results from previous studies that also sug-
277 gest that many parts of Sub-Saharan Africa and Southeast Asia are particularly at risk of high
278 fire-attributable mortality.^{10,23,24}

279 While particulate matter exposure is a known driver of poor infant health outcomes, the extent
280 to which biomass burning drives these effects is not clear. To assess biomass’s contributions to
281 total PM_{2.5} impacts we combine our estimates of biomass-burning-attributable infant deaths
282 with estimates from the Global Burden of Disease (GBD)⁴⁶ on attributable infant deaths from
283 all PM_{2.5} sources to estimate the share of overall PM_{2.5} deaths attributable to biomass burning.
284 We calculate that biomass fires contribute an average of 15.4 percent of total PM infant deaths at
285 the country level over the 2004 to 2018 period (Extended Data Fig 12a). Globally, while PM_{2.5}-
286 related infant deaths have been declining, infant deaths due to biomass fires have been on the rise
287 (Extended Data Fig 12b). As a result, again based on GBD estimates of total infant deaths at-
288 tributable to all PM_{2.5} pollution, we calculate that the contribution of biomass fires to overall
289 PM-related infant deaths has risen from 11 percent in 2004 to over 21 percent by 2018 (Extended
290 Data Fig 12c).

291 Our results additionally suggest that the negative health impacts of biomass burning likely dom-
292 inate any potential health benefits associated with economic activity that generates the anthro-
293 pogenic biomass fires. The coefficient on the downwind burned area which captures the poten-
294 tial local economic benefits of burning is close to zero (Fig 2c). In cross-sectional analysis, we
295 also do not find any evidence that households that are located in places with high burned areas
296 are wealthier (Extended Data Fig 13). Consistent with other recent empirical studies,^{15–17} we
297 find that the health impacts of biomass burning are concentrated within relatively close proxim-
298 ity to the burning itself. This suggests that jurisdictions that undertake policies to reduce burning

299 within a locality will likely also be the primary beneficiaries of that policy in terms of health im-
300 provements. This stands in contrast to perhaps more challenging policy settings such as large
301 wildfires or Saharan dust, in which transboundary movement of pollutants are a substantial source
302 of health impacts.^{27,41,47}

303 Finally, global fire model simulations project an increase in fire activity and burned area in the
304 near future due to human activities and temperature-driven increases linked to climate change.^{48,49}
305 These projected increases have the potential to reverse the decline in burned area observed in re-
306 cent years. Our results suggest that such increases in burned areas would accelerate the contri-
307 bution of outdoor biomass fire exposure to air pollution-related infant deaths and worsen overall
308 infant mortality. Policies to mitigate anthropogenic fire activity, therefore, offer great promise for
309 improving global health outcomes.

310 **References**

- 311 [1] Tami C. Bond, David G. Streets, Kristen F. Yarber, Sibyl M. Nelson, Jung Hun Woo, and
312 Zbigniew Klimont. A technology-based global inventory of black and organic carbon emis-
313 sions from combustion. *Journal of Geophysical Research: Atmospheres*, 109(D14):14203,
314 jul 2004.
- 315 [2] Jianmin Chen, Chunlin Li, Zoran Ristovski, Anđelija Milic, Yuantong Gu, Mohammad S.
316 Islam, Shuxiao Wang, Jiming Hao, Hefeng Zhang, Congrong He, Hai Guo, Hongbo Fu,
317 Branka Miljevic, Lidia Morawska, Phong Thai, Yun Fat LAM, Gavin Pereira, Aijun Ding,
318 Xin Huang, and Umesh C. Dumka. A review of biomass burning: Emissions and impacts
319 on air quality, health and climate in China. *Science of The Total Environment*, 579:1000–
320 1034, feb 2017.
- 321 [3] N. Andela, D. C. Morton, L. Giglio, Y. Chen, G. R. van der Werf, P. S. Kasibhatla, R. S.
322 DeFries, G. J. Collatz, S. Hantson, S. Kloster, D. Bachelet, M. Forrest, G. Lasslop, F. Li,
323 S. Mangeon, J. R. Melton, C. Yue, and J. T. Randerson. A human-driven decline in global
324 burned area. *Science*, 356(6345):1356–1362, 2017.
- 325 [4] Matthias Forkel, Wouter Dorigo, Gitta Lasslop, Emilio Chuvieco, Stijn Hantson, Angelika
326 Heil, Irene Teubner, Kirsten Thonicke, and Sandy P Harrison. Recent global and regional
327 trends in burned area and their compensating environmental controls. *Environmental Re-*
328 *search Communications*, 1(5):051005, jun 2019.

- 329 [5] Emilio Chuvieco, M Lucrecia Pettinari, Nikos Koutsias, Matthias Forkel, Stijn Hantson, and
330 Marco Turco. Human and climate drivers of global biomass burning variability. *Science of*
331 *The Total Environment*, 779:146361, 2021.
- 332 [6] Emilio Chuvieco, Florent Mouillot, Guido R van der Werf, Jesús San Miguel, Mihai Tanase,
333 Nikos Koutsias, Mariano García, Marta Yebra, Marc Padilla, Ioannis Gitas, et al. Historical
334 background and current developments for mapping burned area from satellite earth observa-
335 tion. *Remote Sensing of Environment*, 225:45–64, 2019.
- 336 [7] SK Akagi, Robert J Yokelson, Christine Wiedinmyer, MJ Alvarado, JS Reid, Thomas Karl,
337 JD Crounse, and PO Wennberg. Emission factors for open and domestic biomass burning
338 for use in atmospheric models. *Atmospheric Chemistry and Physics*, 11(9):4039–4072,
339 2011.
- 340 [8] Joel S Levine. *Biomass Burning and Global Change: Remote sensing, modeling and inven-*
341 *tory development, and biomass burning in Africa*, volume 1. MIT Press, 1996.
- 342 [9] Ian Colbeck and Mihalis Lazaridis. Aerosols and environmental pollution. *Naturwis-*
343 *senschaften*, 97(2):117–131, 2010.
- 344 [10] Gareth Roberts and MJ Wooster. Global impact of landscape fire emissions on surface level
345 pm_{2.5} concentrations, air quality exposure and population mortality. *Atmospheric Environ-*
346 *ment*, 252:118210, 2021.
- 347 [11] Louis Giglio, James T. Randerson, and Guido R. van der Werf. Analysis of daily, monthly,
348 and annual burned area using the fourth-generation global fire emissions database (gfed4).
349 *Journal of Geophysical Research: Biogeosciences*, 118(1):317–328, 2013.
- 350 [12] Maria Zubkova, Luigi Boschetti, John T. Abatzoglou, and Louis Giglio. Changes in fire ac-
351 tivity in africa from 2002 to 2016 and their potential drivers. *Geophysical Research Letters*,
352 46(13):7643–7653, 2019.
- 353 [13] Christian Lauk and Karl-Heinz Erb. Biomass consumed in anthropogenic vegetation fires:
354 Global patterns and processes. *Ecological Economics*, 69(2):301–309, 2009.
- 355 [14] John T Abatzoglou and A Park Williams. Impact of anthropogenic climate change on
356 wildfire across western us forests. *Proceedings of the National Academy of Sciences*,
357 113(42):11770–11775, 2016.
- 358 [15] Marcos A Rangel and Tom S Vogl. Agricultural fires and health at birth. *Review of Eco-*
359 *nomics and Statistics*, 101(4):616–630, 2019.

- 360 [16] Hemant Kumar Pullabhotla. *Three essays on agriculture, environment and human capital*
361 *formation in India*. PhD thesis, University of Illinois at Urbana-Champaign, 2019.
- 362 [17] Guojun He, Tong Liu, and Maigeng Zhou. Straw burning, pm_{2.5}, and death: evidence from
363 china. *Journal of Development Economics*, 145:102468, 2020.
- 364 [18] Prachi Singh and Sagnik Dey. Crop burning and forest fires: Long-term effect on adolescent
365 height in india. *Resource and Energy Economics*, page 101244, 2021.
- 366 [19] Vera Samburova, Jessica Connolly, Madhu Gyawali, Reddy LN Yatavelli, Adam C Watts,
367 Rajan K Chakrabarty, Barbara Zielinska, Hans Moosmüller, and Andrey Khlystov. Poly-
368 cyclic aromatic hydrocarbons in biomass-burning emissions and their contribution to light
369 absorption and aerosol toxicity. *Science of the Total Environment*, 568:391–401, 2016.
- 370 [20] Gerhard Lammel, A Heil, I Stemmler, Alice Dvorská, and Jana Klánová. On the contribu-
371 tion of biomass burning to pops (pahs and pcdds) in air in africa. *Environmental science &*
372 *technology*, 47(20):11616–11624, 2013.
- 373 [21] Xiaohua Pan, Charles Ichoku, Mian Chin, Huisheng Bian, Anton Darmanov, Peter Colarco,
374 Luke Ellison, Tom Kucsera, Arlindo da Silva, Jun Wang, et al. Six global biomass burning
375 emission datasets: intercomparison and application in one global aerosol model. *Atmo-*
376 *spheric Chemistry and Physics*, 20(2):969–994, 2020.
- 377 [22] Amanda L Johnson, Michael J Abramson, Martine Dennekamp, Grant J Williamson, and
378 Yuming Guo. Particulate matter modelling techniques for epidemiological studies of open
379 biomass fire smoke exposure: a review. *Air Quality, Atmosphere & Health*, 13(1):35–75,
380 2020.
- 381 [23] Tao Xue, Guannan Geng, Jiajianghui Li, Yiqun Han, Qian Guo, Frank J Kelly, Martin J
382 Wooster, Huiyu Wang, Bahabaike Jiangtulu, Xiaoli Duan, et al. Associations between ex-
383 posure to landscape fire smoke and child mortality in low-income and middle-income coun-
384 tries: a matched case-control study. *The Lancet Planetary Health*, 5(9):e588–e598, 2021.
- 385 [24] Fay H Johnston, Sarah B Henderson, Yang Chen, James T Randerson, Miriam Marlier,
386 Ruth S DeFries, Patrick Kinney, David MJS Bowman, and Michael Brauer. Estimated
387 global mortality attributable to smoke from landscape fires. *Environmental health perspec-*
388 *tives*, 120(5):695–701, 2012.
- 389 [25] David James Purslove Barker, Renate L Bergmann, Pearay L Ogra, et al. *The window of*
390 *opportunity: pre-pregnancy to 24 months of age*, volume 61. Karger Medical and Scientific
391 Publishers, 2008.

- 392 [26] Sam Heft-Neal, Jennifer Burney, Eran Bendavid, and Marshall Burke. Robust relationship
393 between air quality and infant mortality in africa. *Nature*, 559(7713):254–258, 2018.
- 394 [27] Sam Heft-Neal, Jennifer Burney, Eran Bendavid, Kara K Voss, and Marshall Burke. Dust
395 pollution from the sahara and african infant mortality. *Nature Sustainability*, 3(10):863–871,
396 2020.
- 397 [28] Carly L Reddington, Luke Conibear, Suzanne Robinson, Christoph Knote, Stephen R
398 Arnold, and Dominick V Spracklen. Air pollution from forest and vegetation fires in south-
399 east asia disproportionately impacts the poor. *GeoHealth*, 5(9):e2021GH000418, 2021.
- 400 [29] MO Nawaz and DK Henze. Premature deaths in brazil associated with long-term exposure
401 to pm2. 5 from amazon fires between 2016 and 2019. *GeoHealth*, 4(8):e2020GH000268,
402 2020.
- 403 [30] Laura Kiely, Dominick V Spracklen, Christine Wiedinmyer, Luke Conibear, Carly L Red-
404 dington, Stephen R Arnold, Christoph Knote, Md Firoz Khan, Mohd Talib Latif, Lailan
405 Syaufina, et al. Air quality and health impacts of vegetation and peat fires in equatorial asia
406 during 2004–2015. *Environmental Research Letters*, 15(9):094054, 2020.
- 407 [31] Yusheng Shi, Tsuneo Matsunaga, Makoto Saito, Yasushi Yamaguchi, and Xuehong Chen.
408 Comparison of global inventories of co2 emissions from biomass burning during 2002–
409 2011 derived from multiple satellite products. *Environmental pollution*, 206:479–487, 2015.
- 410 [32] Tianjia Liu, Loretta J Mickley, Miriam E Marlier, Ruth S DeFries, Md Firoz Khan,
411 Mohd Talib Latif, and Alexandra Karambelas. Diagnosing spatial biases and uncertain-
412 ties in global fire emissions inventories: Indonesia as regional case study. *Remote Sensing of*
413 *Environment*, 237:111557, 2020.
- 414 [33] Tao Xue, Guannan Geng, Yiqun Han, Huiyu Wang, Jiajianghui Li, Hong-tian Li, Yubo
415 Zhou, and Tong Zhu. Open fire exposure increases the risk of pregnancy loss in south asia.
416 *Nature communications*, 12(1):1–10, 2021.
- 417 [34] Ageo Mário Cândido da Silva, Gisele Pedroso Moi, Inês Echenique Mattos, and Sandra
418 de Souza Hacon. Low birth weight at term and the presence of fine particulate matter and
419 carbon monoxide in the brazilian amazon: a population-based retrospective cohort study.
420 *BMC pregnancy and childbirth*, 14(1):1–8, 2014.
- 421 [35] Pierre Mouganie, Ruba Ajeeb, and Mark Hoekstra. The effect of open-air waste burning on
422 infant health: Evidence from government failure in lebanon. 2020.

- 423 [36] Benjamin A Jones and Robert P Berrens. Prescribed burns, smoke exposure, and infant
424 health. *Contemporary Economic Policy*, 39(2):292–309, 2021.
- 425 [37] Jiajianghui Li, Tianjia Guan, Qian Guo, Guannan Geng, Huiyu Wang, Fuyu Guo, Jiwei Li,
426 and Tao Xue. Exposure to landscape fire smoke reduced birthweight in low-and middle-
427 income countries: findings from a siblings-matched case-control study. *Elife*, 10:e69298,
428 2021.
- 429 [38] Stephanie M Holm, Mark D Miller, and John R Balmes. Health effects of wildfire smoke in
430 children and public health tools: a narrative review. *Journal of exposure science & environ-
431 mental epidemiology*, 31(1):1–20, 2021.
- 432 [39] Sam Heft-Neal, Anne Driscoll, Wei Yang, Gary Shaw, and Marshall Burke. Associations
433 between wildfire smoke exposure during pregnancy and risk of preterm birth in california.
434 *Environmental Research*, 203:111872, 2022.
- 435 [40] Mona Abdo, Isabella Ward, Katelyn O’Dell, Bonne Ford, Jeffrey R Pierce, Emily V Fis-
436 cher, and James L Crooks. Impact of wildfire smoke on adverse pregnancy outcomes in
437 colorado, 2007–2015. *International journal of environmental research and public health*,
438 16(19):3720, 2019.
- 439 [41] Narayan Sastry. Forest fires, air pollution, and mortality in southeast asia. *Demography*,
440 39(1):1–23, 2002.
- 441 [42] Seema Jayachandran. Air quality and early-life mortality evidence from indonesia’s wild-
442 fires. *Journal of Human resources*, 44(4):916–954, 2009.
- 443 [43] Jie-Sheng Tan-Soo and Subhrendu K Pattanayak. Seeking natural capital projects: forest
444 fires, haze, and early-life exposure in indonesia. *Proceedings of the National Academy of
445 Sciences*, 116(12):5239–5245, 2019.
- 446 [44] Elizabeth Frankenberg, Douglas McKee, and Duncan Thomas. Health consequences of
447 forest fires in Indonesia. *Demography*, 42(1):109–129, 2005.
- 448 [45] Krishna Prasad Vadrevu, Kristofer Lasko, Louis Giglio, Wilfrid Schroeder, Sumalika
449 Biswas, and Chris Justice. Trends in vegetation fires in south and southeast asian countries.
450 *Scientific reports*, 9(1):1–13, 2019.
- 451 [46] Global Burden of Disease Collaborative Network. Global burden of disease study 2017 (gbd
452 2017) results. *Seattle, United States: Institute for Health Metrics and Evaluation (IHME)*,
453 2018.

- 454 [47] Achyuta Adhvaryu, Prashant Bharadwaj, James Fenske, Anant Nyshadham, and Richard
455 Stanley. Dust and death: evidence from the west african harmattan. Technical report, Na-
456 tional Bureau of Economic Research, 2019.
- 457 [48] Olga Pechony and Drew T Shindell. Driving forces of global wildfires over the past mil-
458 lennium and the forthcoming century. *Proceedings of the National Academy of Sciences*,
459 107(45):19167–19170, 2010.
- 460 [49] Chao Wu, Sergey Venevsky, Stephen Sitch, Lina M Mercado, Chris Huntingford, and
461 A Carla Staver. Historical and future global burned area with changing climate and human
462 demography. *One Earth*, 4(4):517–530, 2021.
- 463 [50] ICF International. Demographic and health survey sampling and household listing manual.
464 Technical report, MEASURE DHS,, Calverton, Maryland, U.S.A., 2012.
- 465 [51] Roy Burstein, Nathaniel J Henry, Michael L Collison, Laurie B Marczak, Amber Sligar,
466 Stefanie Watson, Neal Marquez, Mahdieh Abbasalizad-Farhangi, Masoumeh Abbasi, Foad
467 Abd-Allah, et al. Mapping 123 million neonatal, infant and child deaths between 2000 and
468 2017. *Nature*, 574(7778):353–358, 2019.
- 469 [52] Institute for Health Metrics and Evaluation. Low- and middle-income country neonatal,
470 infant, and under-5 mortality geospatial estimates 2000-2017. *GHDx*, 2019.
- 471 [53] National Institute of Statistics and Geography (INEGI). Registros administrativos - estadísti-
472 cas. 2020.
- 473 [54] Turkey Statistical Institute Data Portal for Statistics. Infant mortality rate by province 2009-
474 2019. 2019.
- 475 [55] Yanping Wang, Xiaohong Li, Maigeng Zhou, Shusheng Luo, Juan Liang, Chelsea A Lid-
476 dell, Matthew M Coates, Yanqiu Gao, Linhong Wang, Chunhua He, et al. Under-5 mortality
477 in 2851 chinese counties, 1996–2012: a subnational assessment of achieving mdg 4 goals in
478 china. *The Lancet*, 387(10015):273–283, 2016.
- 479 [56] Institute for Health Metrics and Evaluation (IHME). Global burden of disease study 2017
480 (gbd 2017) all-cause mortality and life expectancy 1950-2017. 2019.
- 481 [57] WorldPop. Population counts. 2016. , [https://www.worldpop.org/methods/
482 populations](https://www.worldpop.org/methods/populations).

- 483 [58] Gonzalo Otón, Joshua Lizundia-Loiola, M Lucrecia Pettinari, and Emilio Chuvieco. De-
484 velopment of a consistent global long-term burned area product (1982–2018) based on
485 avhrr-ldtr data. *International Journal of Applied Earth Observation and Geoinformation*,
486 103:102473, 2021.
- 487 [59] Gonzalo Otón. Esa climate change initiative–fire_cci d4. 2.2 product user guide-avhrr-long
488 term data record (pug-ldtr).
- 489 [60] Gonzalo Otón, Rubén Ramo, Joshua Lizundia-Loiola, and Emilio Chuvieco. Global detec-
490 tion of long-term (1982–2017) burned area with avhrr-ldtr data. *Remote Sensing*, 11(18),
491 2019.
- 492 [61] Gonzalo Otón, Magi Franquesa, Joshua Lizundia-Loiola, and Emilio Chuvieco. Validation
493 of low spatial resolution and no-dichotomy global long-term burned area product by pareto
494 boundary. In *Earth Resources and Environmental Remote Sensing/GIS Applications XII*,
495 volume 11863, pages 293–299. SPIE, 2021.
- 496 [62] Ruben Ramo, Ekhi Roteta, Ioannis Bistinas, Dave van Wees, Aitor Bastarrika, Emilio
497 Chuvieco, and Guido R van der Werf. African burned area and fire carbon emissions are
498 strongly impacted by small fires undetected by coarse resolution satellite data. *Proceedings*
499 *of the National Academy of Sciences*, 118(9), 2021.
- 500 [63] Hans Hersbach, Bill Bell, Paul Berrisford, Shoji Hirahara, András Horányi, Joaquín Muñoz-
501 Sabater, Julien Nicolas, Carole Peubey, Raluca Radu, Dinand Schepers, et al. The era5
502 global reanalysis. *Quarterly Journal of the Royal Meteorological Society*, 146(730):1999–
503 2049, 2020.
- 504 [64] Marshall Burke, Erick Gong, and Kelly Jones. Income shocks and hiv in africa. *The Eco-*
505 *nomic Journal*, 125(585):1157–1189, 2015.

506 **Methods**

507 **Infant mortality data.** Data on infant mortality outcomes used in the estimation sample are
508 drawn from births data in the Demographic and Health Surveys (DHS). The DHS are nationally
509 representative surveys conducted in many low and middle-income countries worldwide. Surveyed
510 households are selected using a two-stage sampling procedure. DHS first selects enumeration ar-
511 eas (or clusters), usually drawn from the most recent population census. Within each enumeration
512 cluster, DHS then selects a random set of survey participants based on a listing of all households
513 within the sample enumeration area. The survey interviews all women aged 15-49 in the selected
514 households.⁵⁰ In addition to a number of health-related information, for each woman interviewed,
515 the DHS records their complete birth histories, including the month and year of birth for each
516 child ever-born, the mortality outcome for each birth, and the age of death if the child has not
517 survived. The DHS also provides the geographic coordinates for the primary enumeration sam-
518 ple cluster for most survey rounds. We construct a monthly time series of births recorded at each
519 cluster location using these recalled birth histories data and location information. Our primary
520 outcome variable is a binary indicator taking the value one if the child was reported to have died
521 within 12 months after birth. We use data on the births recorded in all available DHS rounds oc-
522 ccurring between 2004 to 2018 (Extended Data Table 1). Our final sample consists of 2,237,307
523 births, and the mean sample infant mortality rate is 53 deaths per 1000 births.

524 In addition to the DHS births data used in the estimation, we also construct a new harmonized
525 dataset of sub-national infant mortality rates to calculate the number of attributable deaths due to
526 fire smoke globally. To generate the IMR estimates, we utilize a gridded data product published
527 by the IHME (Institute for Health Metrics and Evaluation) in a 2019 study,^{51,52} with IMR esti-
528 mates at a 5kmX5km spatial resolution, and estimates and vital statistics of countries not in the
529 IHME product.⁵³⁻⁵⁵ The IHME product does not cover all the countries in our prediction sam-
530 ple due to several reasons. For example, the list excludes Brazil and Mexico due to the availabil-
531 ity of vital statistics, and China and Turkey due to middle-high SDI (Socio-Demographic Index)
532 score.⁵¹ To generate the estimates for the countries not included in the IHME product, we utilize
533 vital statistics for Turkey,⁵⁴ Mexico,⁵³ state-level IHME estimates for India,⁵² 2017 GBD study
534 estimates for Brazil,⁵⁶ and a study on child mortality in China.⁵⁵ For Brazil and China estimates,
535 we could only obtain under-5 mortality estimates. To generate the IMR estimates, we calculate
536 the national level ratio of IMR-to-Under 5 mortality and scale down the Under-5 mortality esti-
537 mates for each unit (counties for China and states for Brazil) by multiplying the mortality esti-
538 mate by the ratio. Finally, not all datasets cover the full extent of the study period. As a result, we
539 extrapolate the estimates where necessary to generate the IMR estimates for the missing years. To

540 utilize the study estimates of IMR effects in calculating the attributable number of deaths glob-
541 ally, we need an inclusion criterion that ensures the extended sample fall within the distribution
542 of the observed range of infant mortality rates observed in the DHS estimation sample. The out-
543 of-sample country is included in our prediction sample if 90% or more of its IMR estimates fall
544 within the 5th and 95th percentiles of our estimation sample countries' estimates.

545 We use these data to construct a panel of yearly infant mortality rates at a 5 km grid-cell level.
546 We combine these data with estimates of annual number of births within each grid cell con-
547 structed from WorldPop,⁵⁷ and the annual outdoor biomass burned area. We also limit our coun-
548 terfactual scenario estimates to countries that have ranges of burned area and infant mortality
549 within the supports of our DHS-based estimation sample (Extended Data Fig 10). 105 countries
550 met both of these criteria and were included in our analysis. Collectively, these 105 countries ac-
551 count for 98% of total infant deaths during our study period. To construct the annual births coun-
552 try level totals, we first utilized the WorldPop's 2015 gridded data product to assign each grid a
553 percentage of total births that occurred in the country that the cell falls into. After obtaining the
554 percentage we then utilized a country level world births UN data set to compute the number of
555 annual births for the year falling within the study period (2003-2018), by multiplying the percent-
556 age of total births that occurred in country according to WorldPop 2015 gridded estimates by the
557 total births in that year.

558 **Burned area data.** We estimate exposure to outdoor biomass burning using burned area data
559 from the European Space Agency Climate Change Initiative fire data product. Specifically, we
560 use the LTDR Fire_cci version 1.1 pixel product (FireCCILT11) on monthly global burned area.
561 FireCCILT11 provides burned area data at 0.05-degree (≈ 5 km) spatial resolution based on Ad-
562 vanced Very High Resolution Radiometer (AVHRR) imagery.⁵⁸⁻⁶⁰ Validation studies shows that
563 FireCCILT11 provides consistent and accurate estimates of burned area over a long time period.⁶¹
564 We also find good agreement in the overall and regional trends observed using the FireCCILT11
565 with other sources of burned area over the study period. Each birth in our estimation sample, on
566 average, is exposed to 11.5 square kilometers of outdoor biomass burned area per month during
567 pregnancy and in the 12 months after birth (within a 30 km radius around the birth location). Re-
568 cently, products incorporating small fires show more burned area than previous products, but the
569 general spatial distribution across products is found to be similar.⁶² If locations with a higher
570 burned area in our sample are also likely to have more small fires, then our estimates reflect the
571 overall impact of both small and large fires. Empirically, we are also constrained by the limited
572 temporal and spatial coverage of burned area products that account for small fires.

573 **Weather data.** Monthly data on precipitation, temperature, wind direction and wind speed
 574 come from the fifth generation of European ReAnalysis (ERA5) data. ERA5 data provide global
 575 climate reanalysis variables at a 30-km grid, at three hourly intervals.⁶³ The data was downloaded
 576 from the Copernicus Climate Change Service (C3S) Climate Data Store. We use the aggregated
 577 monthly products and extract the weather variables at the location of each birth for the pre- and
 578 post-birth months.

579 **Construction biomass burning exposure.** Using the wind direction at the location of each
 580 birth, we identify up and down-wind quadrants for each month during pregnancy and in the 12
 581 months after birth. The “upwind” quadrant refers to the direction from which wind is blowing to
 582 the birth location, while the “downwind” quadrant is where the wind is blowing away from the
 583 birth location (Extended Data Fig 2). We then calculate the outdoor biomass burned area in the
 584 up and downwind quadrants. Our main estimates use burned areas within a 30 km radius around
 585 the birth location. Results from using burned areas within other distances are shown in the ro-
 586 bustness tests. Using the 30 km radius, we estimate an average upwind burned area of 2.9 km^2
 587 per month and an almost similar amount of 2.8 km^2 of downwind burned area. On average, up-
 588 wind burned area forms about 25% of the total burned area in the births regression sample. To
 589 ease data processing, we use this proportion to approximate the amount of upwind burned area
 590 exposure around the grid cells in the extended sample. We calculate the total burned area around
 591 each grid cell and assign one-fourth of this to be in the upwind direction.

592 **Air pollution ground station monitoring data.** Data on monthly particulate matter pollution
 593 ($PM_{2.5}$) measured at ground station monitors is drawn from daily recorded $PM_{2.5}$ measurements
 594 collected by monitors in the openAQ database (<https://openaq.org>). We subset the data to
 595 stations located in low and middle-income countries as these are more likely to reflect pollution
 596 sources and pollution levels that represent the births sample used in our estimates. Our final sam-
 597 ple consists of 2040 monitors and has an average monthly $PM_{2.5}$ of $48.2 \mu\text{g}/\text{m}^3$. Similar to the
 598 births data, we extract monthly weather variables and calculate up and down-wind burned areas at
 599 each ground station monitor using ERA5 and FireCCILT11 data.

Empirical strategy. We use the following regression model to estimate the effect of burned area exposure on infant mortality:

$$\begin{aligned}
 y_{i,c,g,m,y} = & \sum_d \beta_{1,d} BA_{up,d,i,c,m,y}^{pre} + \sum_d \beta_{2,d} BA_{up,d,i,c,m,y}^{post} \\
 & + \sum_d \beta_{3,d} BA_{down,d,i,c,m,y}^{pre} + \sum_d \beta_{4,d} BA_{down,d,i,c,m,y}^{post} \\
 & + \delta \mathbf{X}_{i,c,g,m,y} + \mu_c + \lambda_{g,m} + \delta_{g,y} + \varepsilon_{i,c,g,m,y}
 \end{aligned} \tag{1}$$

600 where the outcome variable is an indicator for birth i , in cluster c located within country g , oc-
 601 ccurring in month m and year y resulting in a death within 12 months of birth. BA^{pre} and BA^{post}
 602 are, respectively, burned area (in km^2) for the 9 months before and 12 months after birth (includ-
 603 ing month of birth). The sub-scripts up, d and $down, d$ refer, respectively, to the burned area in
 604 upwind and downwind directions in distance bins d around cluster c corresponding to each birth.
 605 We use burned area within 0 – 30, 30 – 40, and 40 – 50 km radii around each cluster to flexibly
 606 allow for burned area effect to vary by distance. Up and downwind exposure refer to the outdoor
 607 biomass burned areas in the up and downwind quadrants (Extended Data Fig 2), measured as the
 608 average monthly burned area in square kilometers during pre-birth and post-birth periods. We in-
 609 clude a set of individual and household characteristics $\mathbf{X}_{i,c,g,m,y}$ such as child gender and birth or-
 610 der, age and education of the mother, as well as weather variables (quadratic polynomials of tem-
 611 perature, precipitation, and wind speed, and wind-direction). Our regression include $\mu_c, \lambda_{g,m}$, and
 612 δ_y , respectively, DHS cluster, country by birth month and country by year of birth fixed effects.
 613 We weight observations by the product of survey-specific household survey weights (supplied by
 614 DHS) and country population weights in order to generate estimates that are representative of the
 615 54 countries across our sample.^{26,64} Our results show that pre-birth exposure does not substan-
 616 tially impact mortality risk, and the impacts are driven primarily by the post-birth exposure to
 617 biomass burned area within the 0-30 km in the upwind direction (Extended Data Fig 3).

Using a similar regression model, we estimate the impact of up and downwind burned areas on
 monthly particulate pollution $PM_{2.5}$ measured at ground station monitors located in low and
 middle-income countries.

$$\begin{aligned}
 PM_{2.5_{i,t}} = & \sum_d \beta_{1,d} BA_{up,i,t} + \sum_d \beta_{2,d} BA_{down,it} \\
 & + \delta \mathbf{X}_{i,t} + \mu_i + \lambda_t + v_{i,t}
 \end{aligned} \tag{2}$$

618 The outcome here is monthly average $PM_{2.5}$ in micrograms per cubic meter at ground station
 619 monitor i in month-year t . We calculate the monthly burned area around each ground station
 620 monitor in up and down-wind directions within the same distance bins as we use in the infant
 621 mortality regression in equation 1. We estimate the effect of outdoor biomass burning on particu-
 622 late pollution using a fixed effects regression model with location and month fixed effects μ_i and
 623 λ_t , respectively. These fixed effects account for any unobserved, time-invariant factors specific to
 624 monitor locations, and shocks common to each month. We also include a vector of weather con-
 625 trols (precipitation, temperature, and wind variables) to account for local climatic conditions that
 626 may be correlated with $PM_{2.5}$ at the ground stations. We find that, similar to the infant mortal-
 627 ity effect, burned area within the 0-30 km in the upwind direction results in an increase in $PM_{2.5}$

628 levels (Extended Data Fig 6).

629 We also examine the sensitivity of the infant mortality and particulate pollution regressions to
630 the radius used to compute burned area radius. Our central estimates use a 30 km radius to define
631 nearby burning. We vary this radius in 5-km increments from 25 to 40 km for infant mortality
632 and the pollution model (Extended Data Fig 7). Overall, the point estimates remain stable across
633 the definitions of nearby burning, with a slight decrease in magnitude as we increase the radius.
634 The coefficient point estimates become less precise as the exposure distance becomes too nar-
635 row or wide. Using a smaller radius (0-25 km) reduces the sample exposure measure’s variation,
636 increasing the standard errors. On the other hand, as the exposure buffer widens (0-40 km), we
637 increase the likelihood of measurement error in the upwind exposure, which attenuates the point
638 estimates and reduces precision.

639 The key takeaway is that we observe a similar diminishing effect of burning with distance for
640 pollution and infant mortality models (Extended Data Fig 7). The remarkably identical pattern
641 we observe for both outcomes lends further support to pollution being the primary mechanism
642 through which outdoor biomass burning affects infant mortality: burning that occurs further away
643 has less impact on particulate air pollution and, therefore, has a smaller effect on health.

To estimate the moderating effect of baseline infant mortality, ambient baseline $PM_{2.5}$, or wealth levels, we interact linear post-birth exposure within 0-30 km with the respective variables:

$$\begin{aligned} y_{i,c,g,m,y} = & \alpha_1 BA_{up,0-30,i,c,m,y}^{post} + \alpha_2 (BA_{up,0-30,i,c,m,y}^{post} \times Z_i) \\ & + \alpha_3 BA_{down,0-30,i,c,m,y}^{post} + \alpha_4 (BA_{down,0-30,i,c,m,y}^{post} \times Z_i) + \\ & + \delta \mathbf{X}_{i,c,g,m,y} + \mu_c + \lambda_{g,m} + \delta_y + u_{i,c,g,m,y} \end{aligned} \quad (3)$$

644 where Z_i is the baseline infant mortality (IMR), ambient baseline $PM_{2.5}$, or wealth levels. Base-
645 line IMR is constructed as follows: we take the sample infant mortality rate for the year prior to
646 birth averaged over clusters located within 1-degree grid-cells around each birth location. Base-
647 line $PM_{2.5}$ is similarly constructed as the lagged average $PM_{2.5}$ at 1-degree grid-cells around
648 each birth location. In case of wealth level Z_i is a vector of dummy variables for wealth quintile.
649 We see no significant variation in the impact of burned area across household wealth or baseline
650 pollution levels. However, the impact of upwind burning exposure reduces with an increase in
651 baseline infant mortality (Extended Data Table 3).

652 **Infant mortality attributable to biomass burning globally.** Our model linking infant mortal-
653 ity to nearby burned area is estimated on the sample of observed births in the DHS. In order to

654 better understand the global impacts of biomass burning on infant health, we apply the estimated
655 relationships to the broader sample of 105 countries available in our extended sample
656 at 5-km grid cell level. We derive infant mortality due to burning under three different scenarios
657 where the counterfactual burned area BA_{ct}^{cf} for each grid cell c and year t is defined as: scenario
658 (i) $BA_{ct}^{cf} = 0$ i.e. burned area is eliminated completely, scenario (ii) $BA_{ct}^{cf} = BA_{c0}$ i.e. burned area
659 is fixed at the observed baseline value (the 3-year average from 2001 to 2003), and scenario (iii)
660 $BA_{ct}^{cf} = \min(BA_{ct})$, $2004 < t < 2018$, for each grid cell c , i.e. burned area is reduced to the min-
661 imum observed within each grid cell during the sample period. For each scenario, we calculate
662 ΔIMR_{ct} , the change in IMR for each year in each grid cell owing to changes in the burned area.
663 We start by estimating the counterfactual change in burned area ΔBA_{ct} for each grid cell-year:

$$\Delta BA_{ct} = BA_{ct} - BA_{ct}^{cf} \quad (4)$$

664 where BA_{ct} is the observed burned area and BA_{ct}^{cf} is the counterfactual burned area correspond-
665 ing to each scenario. We then apply the estimated parameters from the regression in Equation 3,
666 the coefficients on upwind post-birth exposure (α_1) and its interaction with baseline infant mor-
667 tality (α_2), to estimate the change in infant mortality. While doing this, we ensure that the prevail-
668 ing infant mortality rate (IMR_{ct-1}) we use reflects the evolution of infant mortality corresponding
669 to the counterfactual scenario in the preceding year. We start by initializing infant mortality rate
670 to IMR_{c0} , the baseline grid cell-level IMR ($t = 0$ corresponds to 2003 in our study period). The
671 attributable change in infant mortality at $t = 1$ is:

$$\Delta IMR_{ct} = \alpha_1 \Delta BA_{ct} + \alpha_2 \Delta BA_{ct} * IMR_{ct-1} \quad (5)$$

672 We then update the measure of prevailing IMR to account for the estimated change in infant mor-
673 tality (ΔIMR_{ct}) under the counterfactual. This updated IMR (IMR_{ct}^{new}) is given by:

$$IMR_{ct}^{new} = \Delta IMR_{ct} + IMR_{ct-1} \quad (6)$$

674 Using the updated IMR, we estimate the change in infant mortality for the next year under the
675 counterfactual change in burned area:

$$\Delta IMR_{ct} = \alpha_1 \Delta BA_{ct} + \alpha_2 \Delta BA_{ct} * IMR_{ct-1}^{new} \quad (7)$$

676 We repeat this process until the last year in our sample (2018) giving us a time series of ΔIMR_{ct}
677 for each grid cell location. We iterate over bootstrapped parameter estimates α_1 and α_2 in equa-
678 tion 3 in order to derive confidence intervals for the location-specific predictions ΔIMR_{ct} . Us-

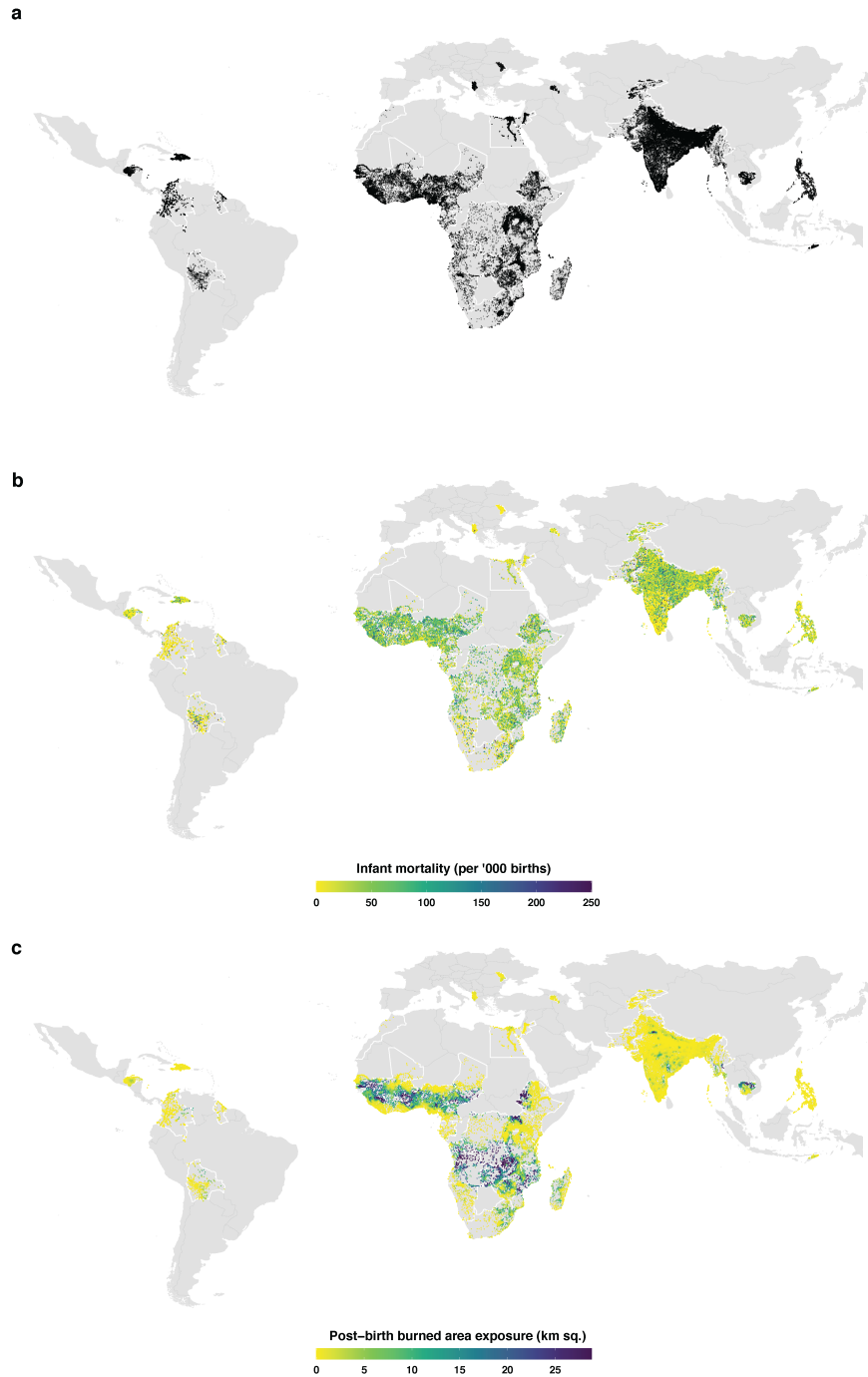
679 ing the observed infant mortality rate and ΔIMR_{ct} , we calculate the share of total infant mortal-
680 ity (S_{ct}) attributable to biomass burning exposure:

$$S_{ct} = \frac{\Delta IMR_{ct}}{IMR_{ct}} \quad (8)$$

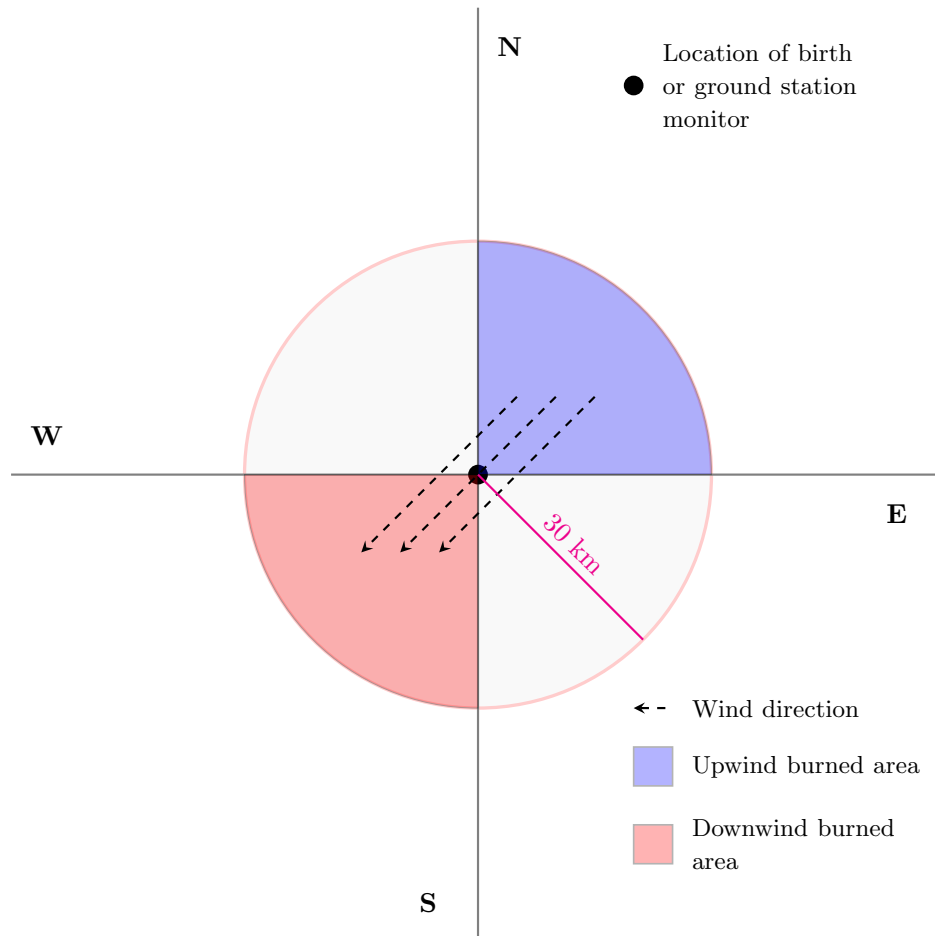
681 Finally, we estimate the number of infant deaths attributable to biomass burning exposure in each
682 location (ID_{ct}):

$$ID_{ct} = \Delta IMR_{ct} \times b_{ct} \quad (9)$$

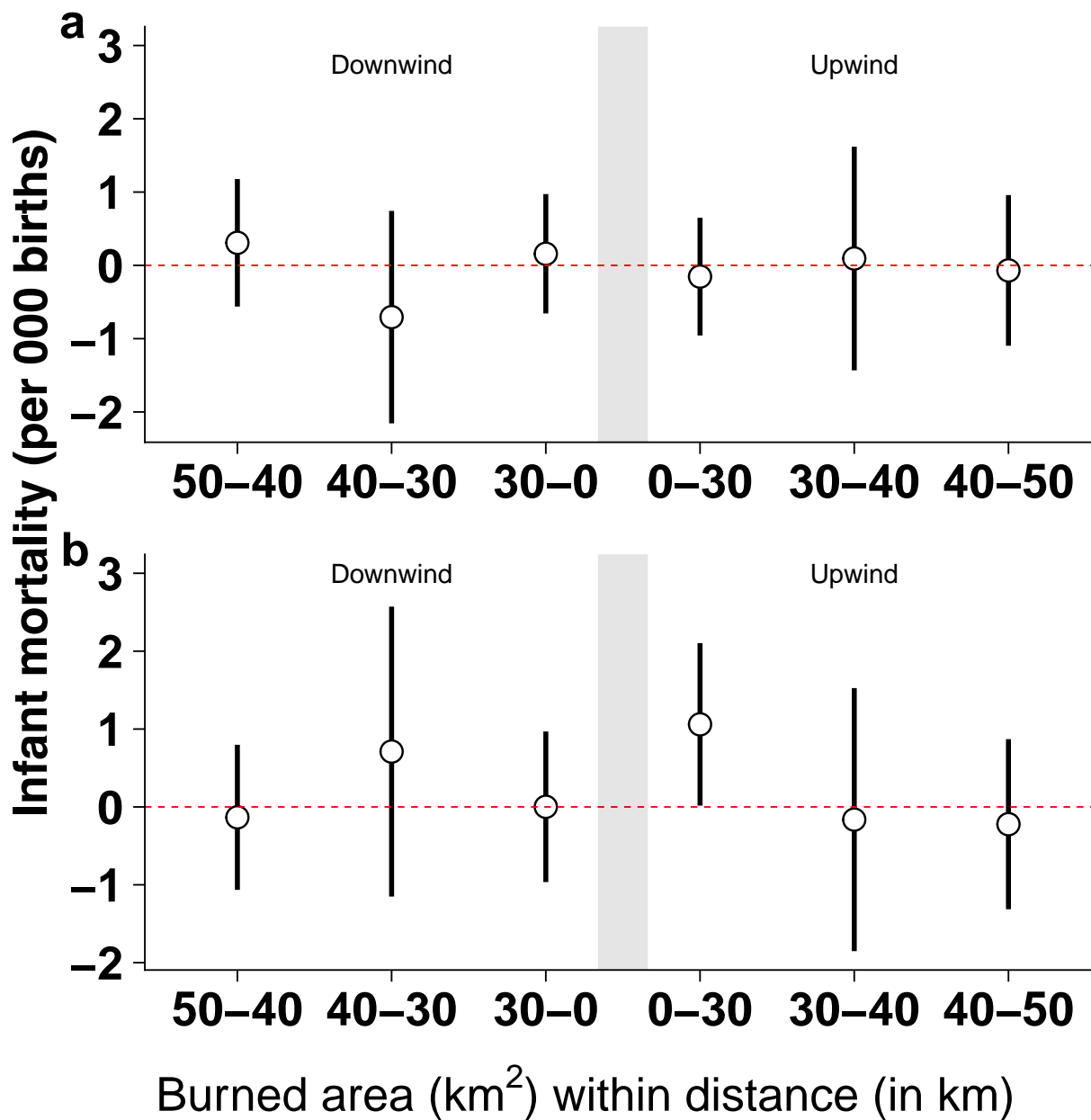
683 where b_{ct} is number of births at location c for year t from WorldPop. For each year, we sum ID_{ct}
684 across all locations to calculate the total number of attributable infant deaths across our extended
685 sample of 105 countries.



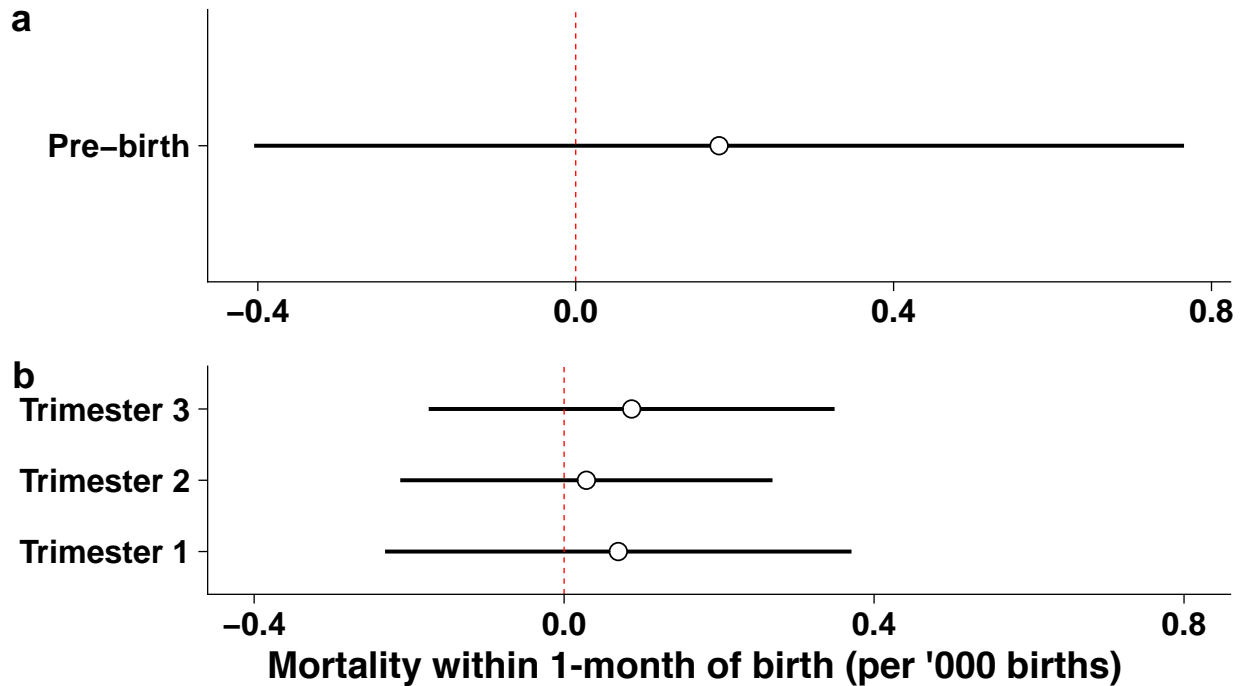
Extended Data Fig 1. | Location of births in estimation sample, average infant mortality and burned area exposure. **a** Location of sample clusters in the DHS data used for estimation ($N = 93063$). DHS data provides geographic coordinates for households at the sample cluster level. **b** Cluster-level sample average infant mortality rate (deaths per '000 births) over the estimation period 2004 - 2018. **c** Cluster-level average post-birth exposure to biomass burned area in (square kilometers per month). Exposure is based on monthly burned area recorded in the up-wind quadrant within a 30 km distance, in the 12 months after birth. The range of values in **b** and **c** are capped at the 99th percentile of the distribution for better visualization. White borders highlight the countries in the DHS births sample used in the estimation.



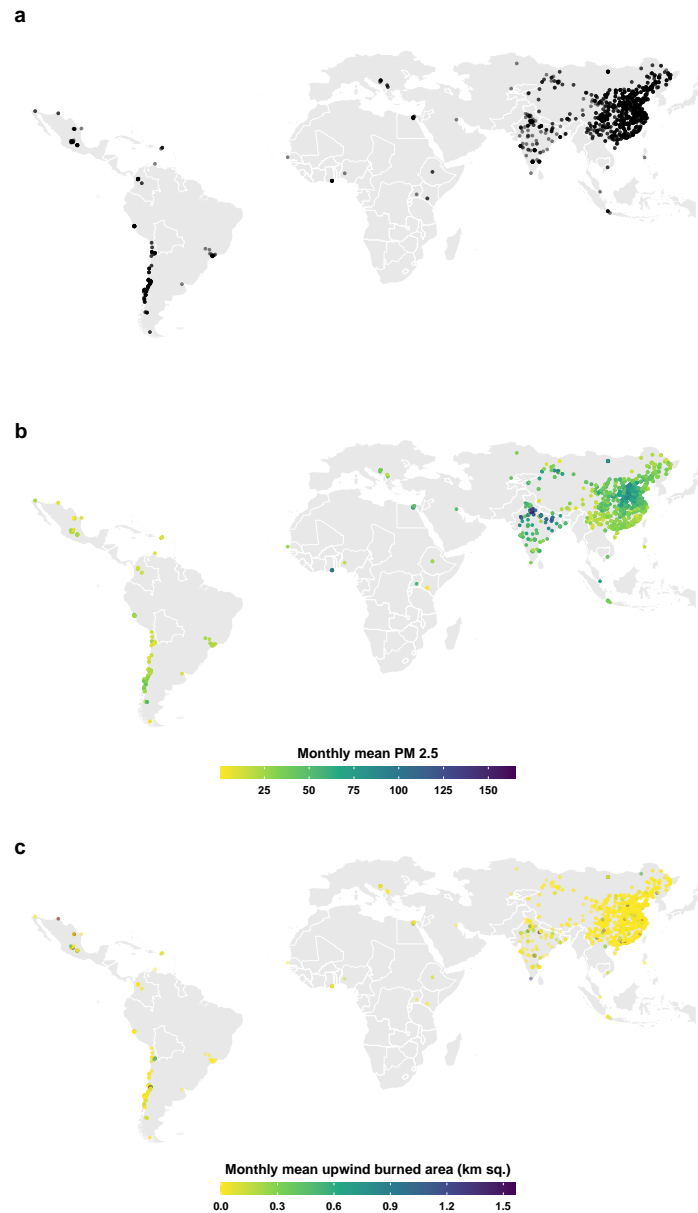
Extended Data Fig 2. | Schematic showing definition of up and downwind burned areas. We estimate exposure to up and downwind biomass burned areas for each birth based on the prevailing wind direction (based on climate reanalysis data) for each month in the pre- and post-birth period. Exposure is calculated by taking the average monthly up and downwind burned areas for the pre- and post-birth periods. In the example shown here, the wind is blowing from the northeast to the southwest. Therefore, upwind (relative to the birth location or ground station monitor) burned area is the biomass burned in the northeast quadrant within a 30-km radius. Biomass burning in the opposing quadrant forms the downwind burned area. The same procedure is used to define up and downwind burned areas around air pollution ground monitors at a monthly resolution. We hypothesize that upwind burned area increases air pollution and result in adverse health outcomes.



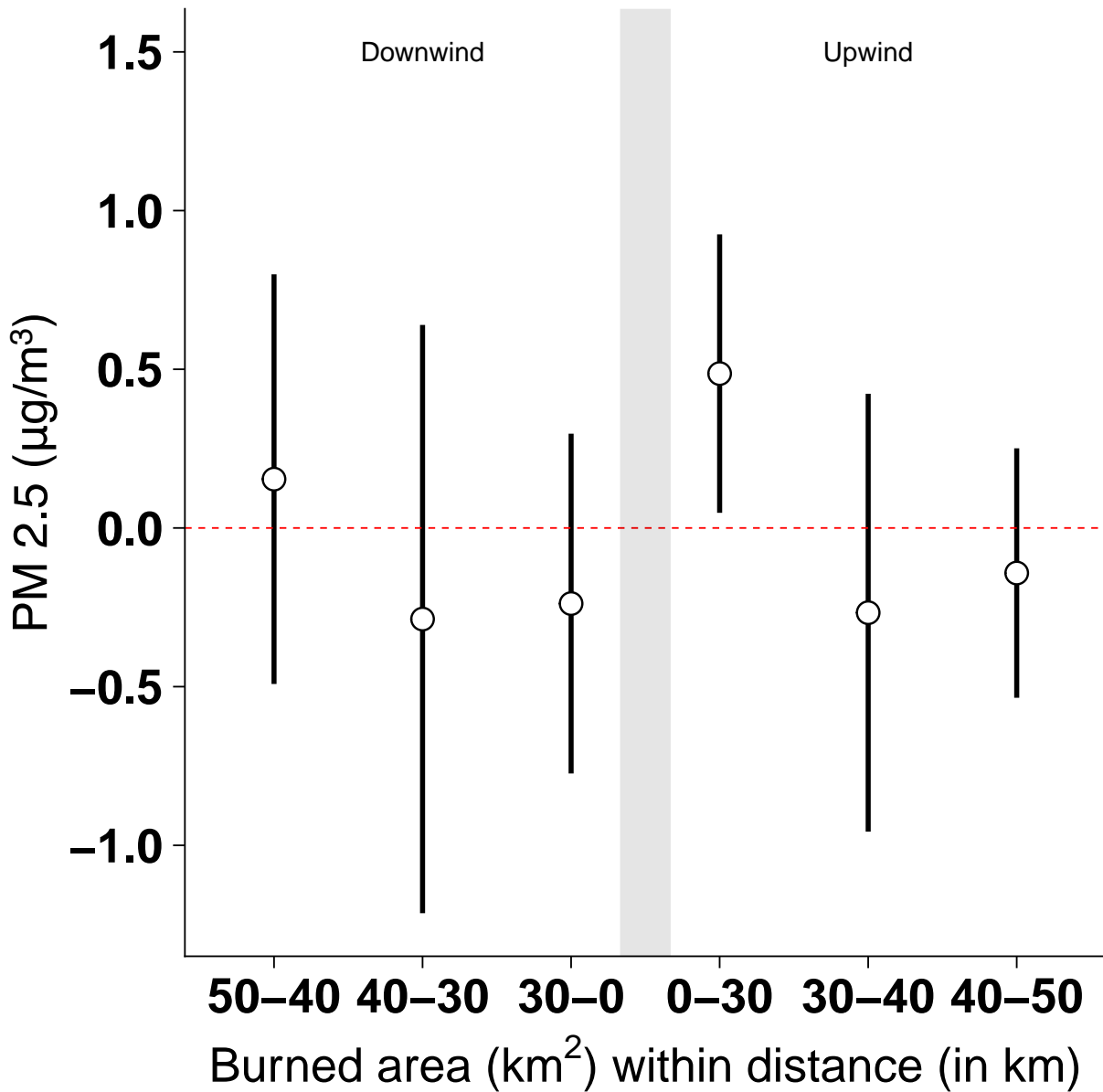
Extended Data Fig 3. | Regression estimates of pre- and post-birth exposure to outdoor biomass burning on infant mortality. **a** and **b** show the coefficient estimates from the regression model in Equation 1 for pre-birth and post-birth exposure, respectively. Circles indicate point estimates, and whiskers the 95% confidence interval on the point estimate. **a** Pre-birth exposure does not have an effect on risk of infant mortality. **b** Post-birth exposure to nearby biomass burning (within 30 km) in the upwind direction increases infant mortality by 1.06 deaths for an additional 1 km^2 increase in burned area. Biomass burning that is further away (30 to 40 or 40 to 50 km) has no effect. Downwind burned areas do not have a significant effect on infant mortality – consistent with pollution from burning blowing away from the location of birth.



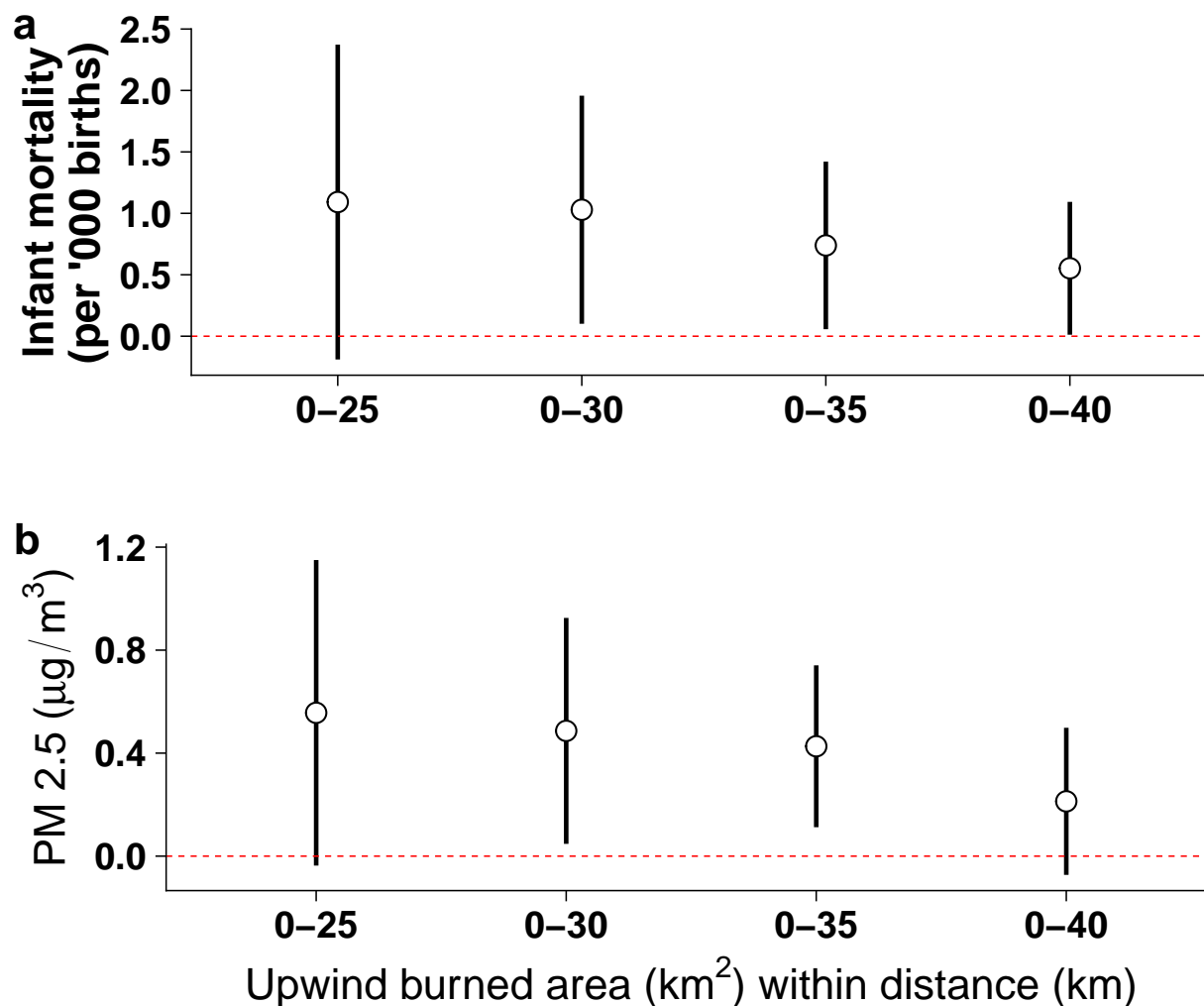
Extended Data Fig 4. | Regression estimates of pre-birth exposure to outdoor biomass burning on mortality within 1-month of birth. a Coefficient estimate on upwind burned area within 0-30 km on mortality within 1-month after birth. **b** Coefficient on trimester-wise upwind burned areas. Circles indicate point estimates, and whiskers the 95% confidence interval on the point estimate. Each plot shows estimates from a separate regression model. Regression specification are similar to Equation 1, but exclude post-birth exposure variables. All other control variables are included in the regressions. **a** shows the estimate from model using average exposure over the whole pre-birth period. **b** uses a model with average exposure within each trimester of the pre-birth period. Sample used is the DHS births data (N = 2.3 million). The sample mean under 1-month mortality is 36.4 deaths per '000 births.



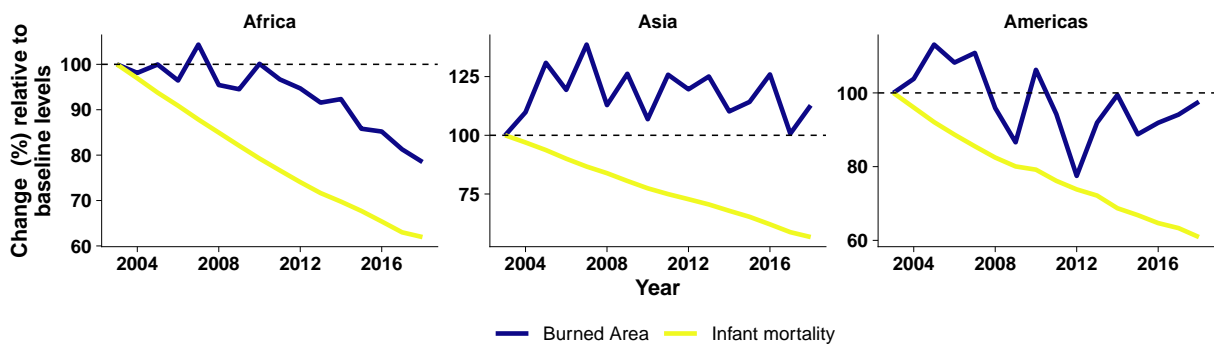
Extended Data Fig 5. | Location, average $PM_{2.5}$ and burned area exposure at ground station monitors. **a** Location of ground station monitors used for estimation ($N = 2040$). **b** Monthly sample average $PM_{2.5}$ ($\mu g/m^3$) from 2014 - 2018 recorded by monitors. **c** Average upwind exposure to biomass burned area in (square kilometers per month). Exposure is based on monthly burned area recorded in the upwind quadrant within a 30 km distance. The range of values in **b** and **c** are capped at the 99th percentile of the distribution for better visualization. White borders highlight the countries in the DHS births sample used in the infant mortality estimation.



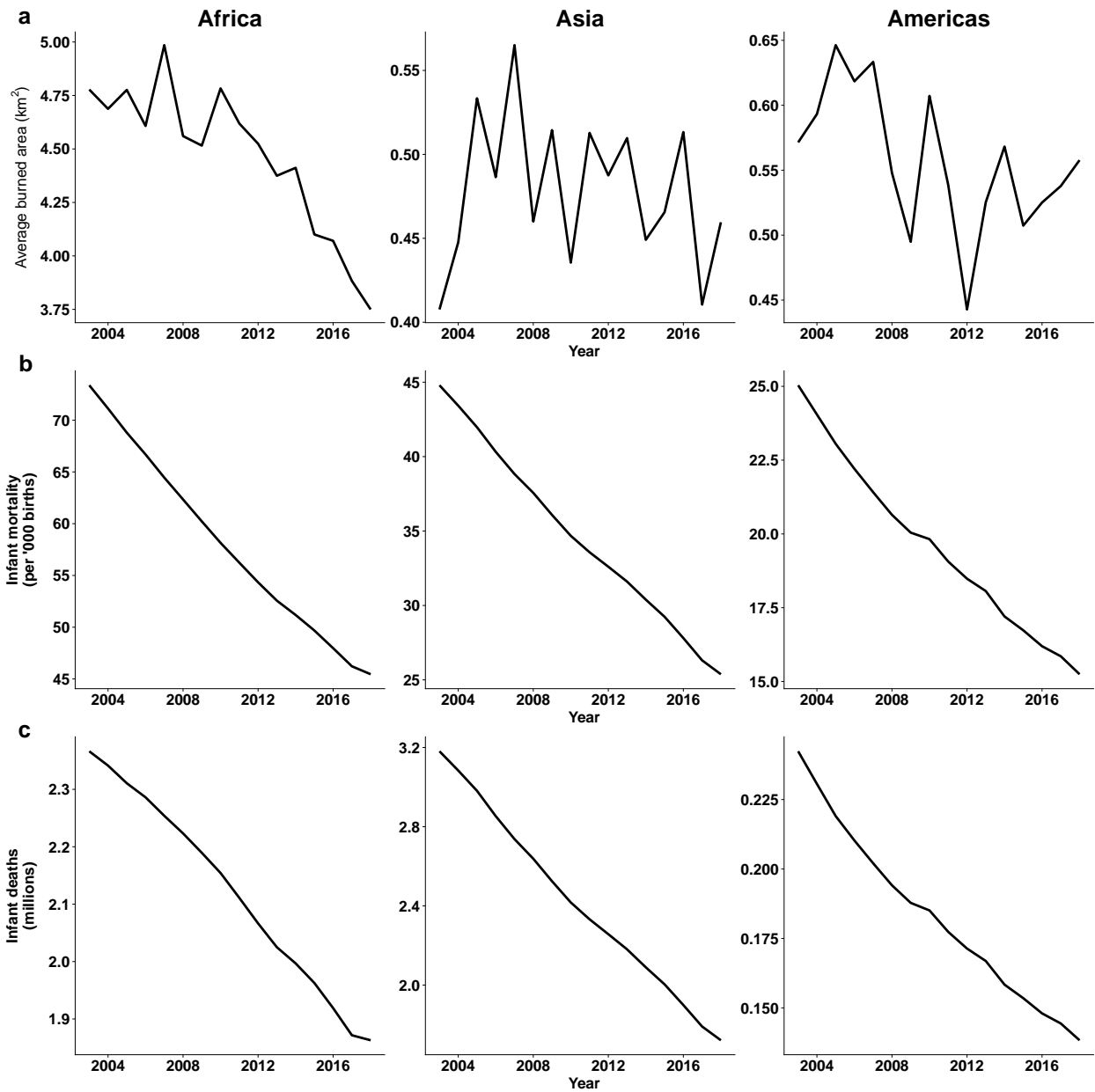
Extended Data Fig 6. | Regression estimates of outdoor biomass burning on $PM_{2.5}$ at ground station monitors. Plot show the coefficient estimates for the impact of monthly burned area in up and downwind directions around ground station monitors on $PM_{2.5}$ recorded at the monitors. Each additional square kilometer increase in nearby biomass burning (within 30 km) in the upwind direction increases $PM_{2.5}$ by $0.49 \mu\text{g}/\text{m}^3$. Biomass burning that is further away (30 to 40 or 40 to 50 km) has no effect. Downwind burned areas do not have a significant effect on $PM_{2.5}$ – consistent with pollution from burning blowing away from the location of the air pollution monitors. Circles indicate point estimates, and whiskers the 95% confidence interval on the point estimate.



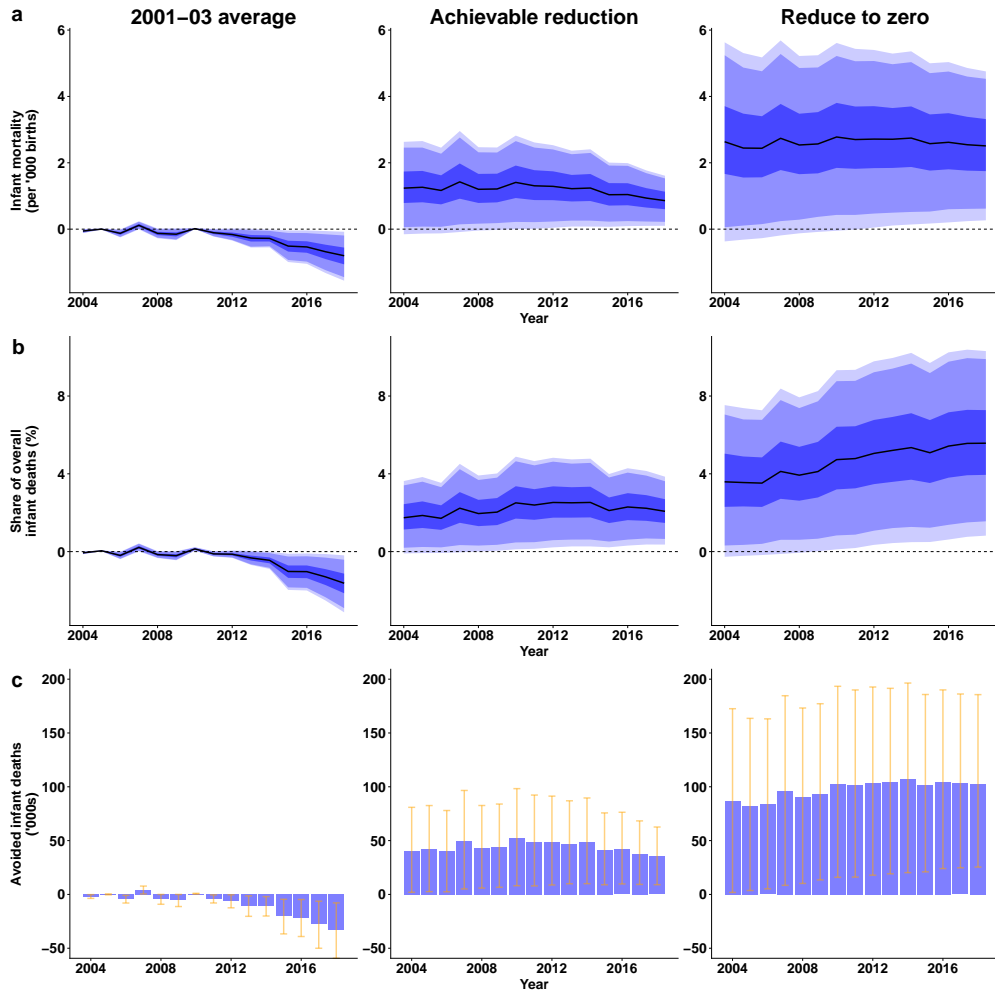
Extended Data Fig 7. | Variation in effect of upwind burned area on infant mortality and particulate pollution using different exposure radii. **a** shows the coefficient estimates of the effect of post-birth upwind burned area exposure on infant mortality. Each coefficient is from a separate regression model. Regression specification are similar to Equation 1, but exclude pre-birth exposure. The effect of each additional square kilometer upwind burned area on infant mortality declines in magnitude as the distance used to define exposure increases. **b** shows the effect of monthly upwind burned area on $PM_{2.5}$ at ground station monitors when distance used to define nearby exposure is changed. Each estimate is from a separate regression model using specifications similar to Equation 2. The effect of each additional square kilometer upwind burned area on $PM_{2.5}$ shows a strikingly similar pattern to that seen in **a** as the distance used to define exposure is varied. Circles indicate point estimates, and whiskers the 95% confidence interval on the point estimate.



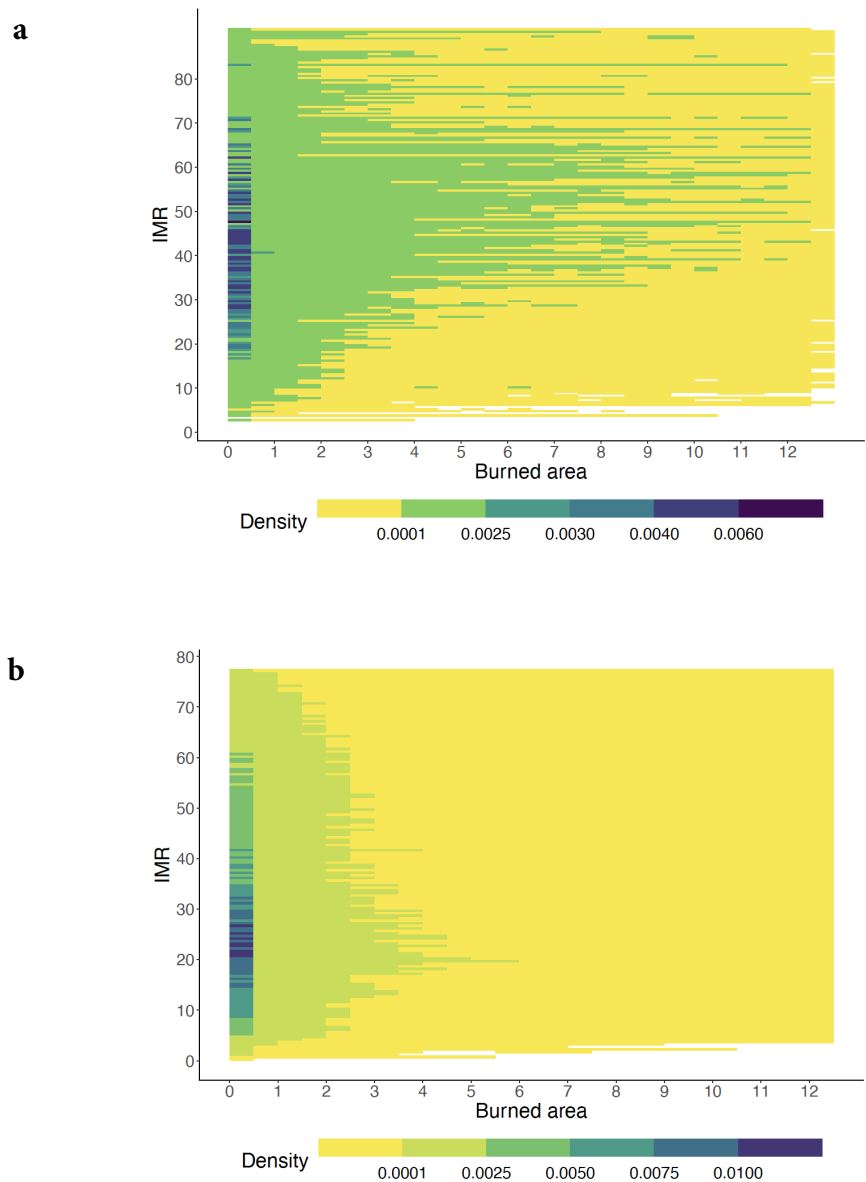
Extended Data Fig 8. | Births-weighted trends in burned area and infant mortality rate by region, relative to baseline values. Plots show the annual birth-weighted average biomass burned area and infant mortality rate, averaged over the 5 km × 5 km grid-cells used in the extended global sample. Annual values are normalized setting baseline values to 100. Baseline values are the 3-year average from 2001-2003 for burned area, and 2003 levels for infant mortality.



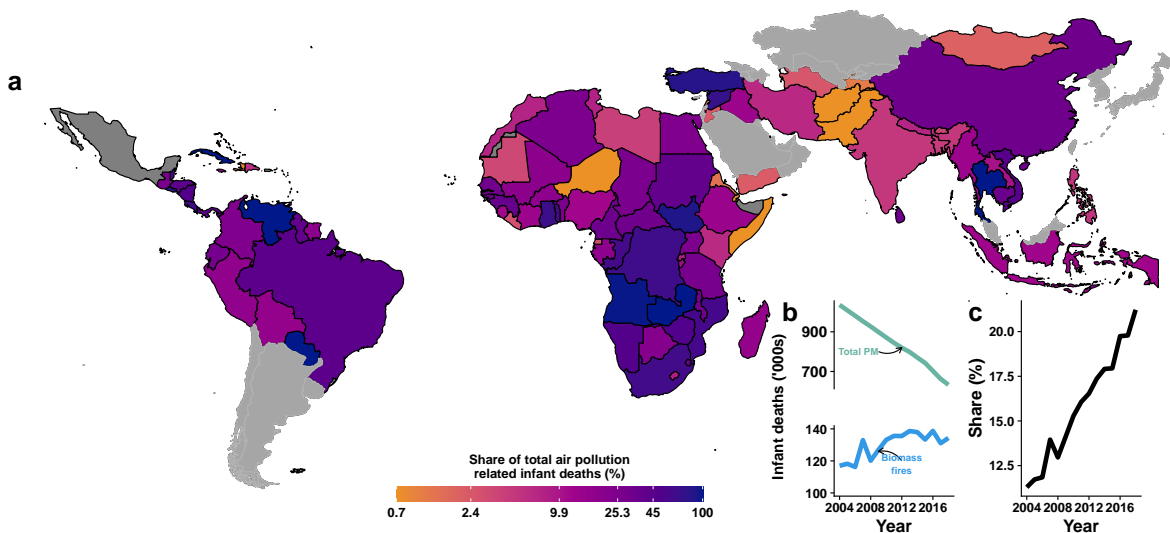
Extended Data Fig 9. | Trends in births-weighted burned area, births-weighted infant mortality rate, and total infant deaths by region in the extended sample. a Annual birth-weighted average upwind biomass burned area and infant mortality rate, averaged over all grid-cells used in extended sample. **b** Annual infant mortality rate (births-weighted average over all grid cells). **c** Total number of infant deaths estimated as the product of infant mortality rate and number of births, summed up over all grid cells in the region for each year.



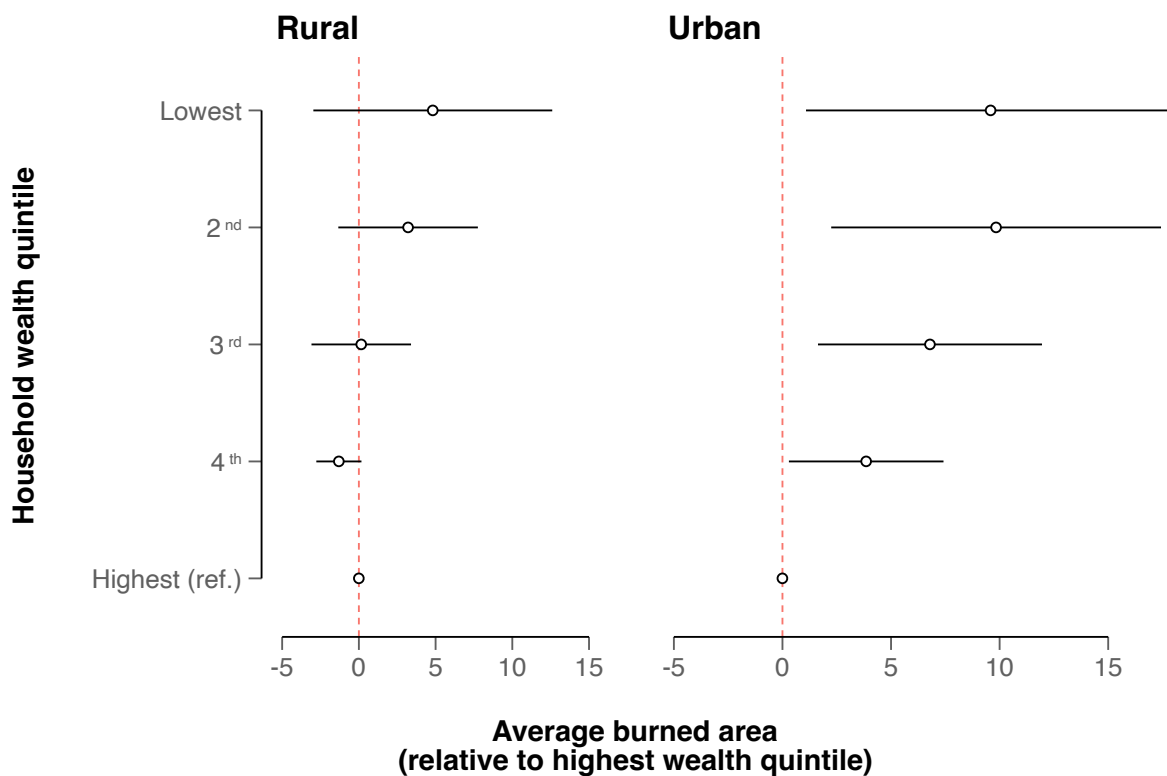
Extended Data Fig 10. | Avoided infant deaths in Africa region from reduced post-birth exposure to outdoor biomass burning under different scenarios. **a**, **b**, and **c**, respectively, show infant mortality attributable to biomass burning exposure, share of overall infant mortality (%), and number of avoided infant deaths for three scenarios, from left to right – burning held at the baseline values, reduced to achievable levels (the minimum observed burned area at each grid cell location during 2004-18), and complete reduction. Shaded regions in **a** and **b** show the 25th to 75th (darkest), 10th to 90th (medium), and 5th to 95th (lightest) percentile ranges based on bootstrapped estimates of predicted infant mortality values at each 1 km X 1 km grid cell, for each year. Error bars in **c** show 5th to 95th percentile range and the bar height represents the median.



Extended Data Fig 11. | Distribution of burned area and infant mortality rates in estimation sample and extended sample . Density of infant mortality and burned area distribution in **a** the DHS births data used in the regression estimates, and **b** in the extended sample used for calculating the global number of attributable deaths.



Extended Data Fig 12. | Share of total air pollution related infant deaths attributable to biomass fires exposure. **a** Share of total infant deaths due to particulate matter pollution (PM) attributable to biomass burning exposure estimated in this study (averaged over the study period 2004 - 2018 within each country in sample). **b** Yearly trend in annual infant deaths attributable to overall PM and the estimated infant deaths due to exposure to biomass fires (annual total across all sample countries). **c** Annual trend in the share of biomass fire exposure in overall PM infant deaths (average across all countries for each year weighted by total PM infant deaths). Overall PM-related infant deaths are based on Global Burden of Disease (GBD) estimates,⁴⁶ calculated as deaths occurring in early, late, or post neonatal age groups due to particulate matter pollution risk. Infant deaths due to biomass fires are estimated by aggregating the grid-cell level estimates from this study to the country-year level.



Extended Data Fig 13. | Cross-sectional relationship between total burned area and household wealth level in rural and urban DHS clusters. We regress the average monthly biomass burned area in the two years preceding the survey year (within a 30-km radius around the households' cluster location) on household wealth quintile indicators, controlling for country and survey year fixed effects.

Extended Data Table 1 | List of DHS surveys in sample

Country	Survey Year(s)	Observations
Albania	2008, 2017	10019
Angola	2006, 2011, 2015	41300
Armenia	2010, 2015	6198
Bangladesh	2004, 2007, 2011, 2014, 2018	61822
Benin	2012, 2017	53518
Bolivia	2008	7203
Burkina Faso	2010	19339
Burundi	2010, 2016	41820
Cambodia	2005, 2010, 2014	29942
Cameroon	2004, 2011, 2018	40862
Chad	2014	41791
Colombia	2010	22678
Comoros	2012	5197
Cote d'Ivoire	2012	12052
Democratic Republic of the Congo	2007, 2013	37141
Dominican Republic	2007, 2013	14218
Egypt	2005, 2008, 2014	43418
Ethiopia	2005, 2010, 2016	44121
Gabon	2012	9358
Ghana	2008, 2014	14971
Guinea	2005, 2012, 2018	34729
Guyana	2009	2145
Haiti	2006, 2012, 2016	30927
Honduras	2011	16612
India	2015	636579
Jordan	2007, 2012, 2017	55610
Kenya	2008, 2014	50950
Kyrgyz Republic	2012	6732
Lesotho	2004, 2009, 2014	11706
Liberia	2007, 2009, 2013	22349
Madagascar	2008	12162

(continued)

Country	Survey Year(s)	Observations
Malawi	2004, 2010, 2015	69101
Mali	2006, 2012, 2018	47963
Moldova	2005	519
Morocco	2003	14
Mozambique	2011	16142
Myanmar	2015	12121
Namibia	2006, 2013	12087
Nepal	2006, 2011, 2016	24257
Nigeria	2008, 2010, 2013, 2018	175957
Pakistan	2006, 2017	33279
Philippines	2008, 2017	34351
Rwanda	2005, 2008, 2010, 2014	37129
Senegal	2005, 2008, 2010	35582
Sierra Leone	2008, 2013, 2019	54215
South Africa	2016	8159
Swaziland	2006	1651
Tajikistan	2012, 2017	21860
Tanzania	2007, 2010, 2015	37567
Timor	2009, 2016	29852
Togo	2013	14010
Uganda	2006, 2009, 2011, 2016	56676
Zambia	2007, 2013, 2018	55338
Zimbabwe	2005, 2010, 2015	22006

Extended Data Table 2 | Regression results for main specification and robustness of post-birth exposure to alternative specifications

Dependent Variable:	Infant mortality (per '000 births)				
	(1)	(2)	(3)	(4)	(5)
<i>Variables</i>					
Upwind exposure, post-birth	1.060** (0.5322)	1.184** (0.5026)	0.9553** (0.4860)	1.038* (0.5408)	1.067** (0.5333)
Downwind exposure, post-birth	0.0018 (0.4932)	0.2519 (0.4735)	0.1143 (0.4535)	-0.1486 (0.4925)	0.0100 (0.4953)
Upwind exposure, pre-birth	-0.1531 (0.4102)	-0.3802 (0.3483)	-0.1374 (0.3580)	-0.1314 (0.4162)	-0.1693 (0.4105)
Downwind exposure, pre-birth	0.1581 (0.4156)	0.2191 (0.3619)	0.0578 (0.4053)	0.1905 (0.4213)	0.1511 (0.4165)
<i>Fixed-effects</i>					
DHS sample cluster	Yes	Yes	Yes	Yes	Yes
Country-Birth month	Yes			Yes	Yes
Country-Birth year	Yes			Yes	Yes
1-degree grid cell × Birth month		Yes			
1-degree grid cell × Birth year		Yes			
2-degree grid cell × Birth month			Yes		
2-degree grid cell × Birth year			Yes		
Observations	2,237,307	2,237,307	2,237,307	2,237,307	2,237,307

Table shows estimates from separate regressions in each column. Regression models are based on the specification shown in Equation 1. Up and downwind exposure refer to the outdoor biomass burned area within 0-30 km in the up and downwind quadrants (Extended Data Fig 2), measured as the average monthly burned area in square kilometers during the nine months preceding birth (pre-birth) and the 12 months after birth, including month of birth (post-birth). Column **1** shows the results from the main specification with country by birth month and country by birth year fixed effects. Columns **2** and **3** flexibly control for seasonal and year effects at a finer spatial scale through the use of 1-degree and 2-degree grid cell fixed effects, respectively, instead of country level fixed effects. Column **4** shows the estimates without the inclusion of child, maternal and household control variables. Column **5** excludes climatic factors (temperature, precipitation and wind speed) from the model. Values in parentheses show the standard errors clustered at the DHS sample cluster level. Coefficient significance at 1%, 5% and 10% are indicated by ***, ** and *, respectively.

Extended Data Table 3 | Regression results - heterogeneity in the effect of post-birth upwind burned area by household wealth, baseline infant mortality and baseline particulate pollution

Dependent Variable:	Infant mortality (per '000 births)		
	(1)	(2)	(3)
<i>Variables</i>			
Upwind BA × Wealth Quintile 1	0.8850 (0.5913)		
Upwind BA × Wealth Quintile 2	1.274** (0.6070)		
Upwind BA × Wealth Quintile 3	1.203** (0.5813)		
Upwind BA × Wealth Quintile 4	0.9109 (0.8028)		
Upwind BA × Wealth Quintile 5	0.7809 (0.7829)		
Upwind BA × IMR		-0.0054*** (0.0018)	
Upwind BA × $PM_{2.5}$			-0.0046 (0.0129)
<i>Fixed-effects</i>			
DHS sample cluster	Yes	Yes	Yes
Country-Birth month	Yes	Yes	Yes
Country-Birth year	Yes	Yes	Yes
Wealth quintile	Yes		
Observations	2,237,307	2,237,307	2,237,307

Table shows estimates from separate regressions in each column. Regression models are based on the specification shown in Equation 3. “Upwind BA” refers to average monthly upwind outdoor biomass burned area exposure (in km^2) within 0-30 km distance during the post-birth period. For brevity, each column shows the coefficients on the interaction of post-birth upwind burned area exposure with the modifiers household wealth in column 1, baseline infant mortality rate in column 2, and baseline pollution ($PM_{2.5}$) in column 3. Baseline IMR is constructed as follows: we take the sample infant mortality rate for the year prior to birth averaged over clusters located within 1-degree grid-cells around each birth location. Baseline $PM_{2.5}$ is similarly constructed as the lagged average $PM_{2.5}$ at 1-degree grid-cells around each birth location. Values in parentheses show the standard errors clustered at the DHS sample cluster level. Coefficient significance at 1%, 5% and 10% are indicated by ***, ** and *, respectively.